

**Towards an integrated framework for evidencing demographic buffering in natural populations**

A manuscript in preparation for submission to ECOLOGY LETTERS  
Type of article: METHOD

Gabriel Silva Santos<sup>1,2\*</sup>, Samuel J L Gascoigne<sup>3\*</sup>, André Tavares Corrêa Dias<sup>4</sup>, Maja Kajin<sup>3,5\*\*</sup> ♦, Roberto Salguero-Gómez<sup>3</sup> ♦

<sup>1</sup> National Institute of the Atlantic Forest (INMA), 29650-000, Santa Teresa, Espírito Santo, Brazil. [ssantos.gabriel@gmail.com](mailto:ssantos.gabriel@gmail.com)

<sup>2</sup> Department of Ecology, Graduate Program in Ecology and Evolution, Rio de Janeiro State University, 524 São Francisco Xavier Street, 20550-900, Maracanã, Rio de Janeiro, Brazil.

<sup>3</sup> Department of Biology, University of Oxford, South Parks Road, OX1 3RB, Oxford, UK. [samuel.gascoigne@pmb.ox.ac.uk](mailto:samuel.gascoigne@pmb.ox.ac.uk), [rob.salguero@biology.ox.ac.uk](mailto:rob.salguero@biology.ox.ac.uk)

<sup>4</sup> Department of Ecology, Institute of Biology, Universidade Federal do Rio de Janeiro, Avenida Carlos Chagas Filho 373, 21941-590 Rio de Janeiro, RJ, Brazil. [atcdias@gmail.com](mailto:atcdias@gmail.com)

<sup>5</sup> **Chair of Zoology**, Department of Biology, Biotechnical Faculty, University of Ljubljana, Večna pot 111, 1000 Ljubljana, Slovenia. [maja.kajin@bf.uni-lj.si](mailto:maja.kajin@bf.uni-lj.si)

\*Shared first authorship

\*\*Corresponding author

♦ Shared senior authorship

**AUTHOR CONTRIBUTIONS:** GSS developed the initial concept, performed the statistical analyses, and contributed to the first draft of the manuscript. SJLG developed the initial concept, contributed to the first draft and all other versions of the manuscript, and generated final figures. ATCD co-advised the project and contributed significantly to final versions of the manuscript. MK developed and managed the project, contributed to the first draft and all other versions of the manuscript, and generated final figures. RSG developed and managed the project and contributed to the first draft and all other versions of the manuscript. All authors made substantial contributions to editing the manuscript and further refining ideas and interpretations.

**RUNNING TITLE:** Demographic buffering framework (32/45 characters)

**KEYWORDS:** COMADRE Animal Matrix Database, elasticity, life-history evolution, natural selection, second-order derivative, sensitivity, stochasticity, variance.

**NUMBER OF WORDS:** Abstract – 146/150 words, main text (excluding abstract, acknowledgements, references, table, and figure legends) – 4979/5000 words

**NUMBER OF REFERENCES:** 86

**NUMBER OF TABLES:** 2 (in Supplementary Material)

**NUMBER OF FIGURES:** 3

Deleted: A

Deleted: unified

Deleted: to

Deleted: quantify

Deleted: , maja.kajin@biology.ox.ac.uk

Deleted: 3

Deleted: 4966

Deleted: 60

Deleted: 1

59 **Abstract** (146/150 words)

60 The demographic buffering hypothesis predicts that natural selection reduces the temporal  
61 fluctuations in demographic processes (survival, development, and reproduction) due to their  
62 negative impacts of temporal variation on population dynamics. However, evidencing  
63 buffering patterns at different hierarchical levels – between and within populations – and  
64 understanding how selection shapes those patterns, remains a challenge in Ecology and  
65 Evolution. Here, we introduce a framework that allows for the evidencing of demographic  
66 buffering between and within populations. The framework uses the sum of stochastic  
67 elasticities for between-populations comparisons along with first- and second-order effects of  
68 demographic process variability on fitness for within-population comparisons. We apply this  
69 framework to 43 populations of 37 mammal species to test the hypothesis that buffered  
70 species are under strong concave selection pressures. Using our framework, we show that  
71 demographically buffered species do not necessarily have strong concave selection pressures  
72 in their most impactful demographic processes.

Deleted: ¶

Deleted: 43

Deleted: D

Deleted: B

Deleted: H

Deleted: (DBH)

Deleted: such as

Deleted: ,

Deleted: a comprehensive approach that allows for the examination of demographic buffering patterns across multiple species is still lacking

Deleted: propose

Deleted: that an additional metric - a second-order effect on population growth rate – be added to the framework for evidencing demographic buffering.

Deleted: Firstly, w

Deleted: categorize species along a continuum of variance based on the sums of stochastic elasticities. Secondly, we examine the linear selection gradients, followed by the examination of nonlinear selection gradients as the third step. With these three steps, our framework overcomes existing limitations of conventional approaches to quantify demographic buffering, allows for multi-species comparisons, and offers insight into the evolutionary forces that shape demographic buffering. We apply this framework to mammal species and discuss both the shortagesadvantages and potential of our framework.¶

Environmental stochasticity shapes organisms' life histories (Bonsall & Klug 2011; Stearns 1992; Tuljapurkar 1990, 2010). Nonetheless, how organisms will cope with the changing variation in environmental conditions (Bathiany *et al.* 2018; Boyce *et al.* 2006; Morris *et al.* 2008) remains an intriguing ecological and evolutionary question (Sutherland *et al.* 2013). Evolutionary demography provides diverse explanations for how evolutionary processes shape demographic responses to environmental stochasticity (Charlesworth 1994; Healy *et al.* 2019; Hilde *et al.* 2020; Pfister 1998; Tuljapurkar *et al.* 2009). The long-term stochastic population growth rate, ( $\lambda_s$ ), representing the geometric mean of population growth rates over time ( $\lambda_t$ ; Tuljapurkar 1982), forms the basis of the Demographic Buffering Hypothesis (Morris & Doak 2004; Pélabon *et al.* 2020).

Increasing the geometric mean of  $\lambda_t$  over time corresponds to a rise in the long-term stochastic population growth rate. Conversely, higher variance in  $\lambda_t$  reduces  $\lambda_s$  (Morris & Doak 2004; Tuljapurkar 1982), impacting population persistence (Lefèvre *et al.* 2016). The demographic buffering hypothesis (Pfister 1998) suggests life histories are selected to minimize the negative impacts of environmental variation by constraining the temporal variance of key demographic processes (e.g., survival, development, reproduction) that have the highest sensitivity/elasticity to population growth rate, a fitness proxy (Gaillard & Yoccoz 2003; Pfister 1998). Demographic buffering describes the selection-driven constraint on the temporal variance of these key demographic processes (Gascoigne *et al.* 2024a, b; Hilde *et al.* 2020; Morris & Doak 2004; Pfister 1998). Here, we focus on the emerging patterns of demographic buffering in different animal life histories, rather than on the demographic buffering hypothesis itself.

An integrative approach to evidence demographic buffering is still missing. Indeed, identifying demographic buffering remains challenging (Doak *et al.* 2005; Morris & Doak 2004) for several reasons, one of them being different interpretations of results from

Deleted: increasing

Deleted: ,

Deleted: expressed

Deleted: as

Deleted: annual

Deleted: ,

Deleted: ,

Deleted: (DBH)

Deleted: ( $\lambda_s$ , hereafter)

Deleted: DBH

Deleted: predicts that life histories are under selection pressure to minimise the negative impacts of environmental variation by constraining the temporal variance of those demographic processes (e.g., survival, development, reproduction) to which population growth rate (*i.e.*, a proxy for fitness)

Deleted: is most sensitive

Deleted: to

Deleted:

Deleted: The demographic pattern strategy operating the DBH, *i.e.*, demographic buffering, describes the selection-driven constraint on the temporal variance of the most impacting demographic processes for the population growth rate ...

Deleted: .

Deleted: latter - on the

Deleted: -

Deleted: DBH

Deleted: unified

Deleted: unambiguously

Deleted: quantify

correlational analyses, as in Pfister (1998) and Hilde *et al.* (2020). Some authors rank species' life histories on a continuum from buffered to labile using the correlation coefficient (Spearman's correlation  $\rho$ ) between the impact of demographic processes on the population growth rate and the temporal variance of said demographic processes (McDonald *et al.* 2017; Salguero-Gómez 2021). There, negative correlation coefficient values indicate buffering. Alternatively, the absence of statistical support for buffering may suggest a preference for demographic variance to track environmental conditions, a phenomenon supported by the Demographic Lability Hypothesis (Drake 2005; Hilde *et al.* 2020; Jäkäläniemi *et al.* 2013; Koons *et al.* 2009; Reed & Slade 2012). However, increased variability alone is not enough to constitute demographic lability; it must also result in significant changes in the mean value of the demographic process (Le Coeur *et al.* 2022).

Deleted: (e.g.,

Deleted: Some authors rank species' life histories on a continuum from buffered to labile using the correlation coefficient (Spearman's correlation  $\rho$ ), where negative values indicate buffering (McDonald *et al.* 2017)

Deleted: known as

Deleted: (DLH)

Deleted: temporal variance

Another obstacle to generalising a measure of demographic buffering across populations and species is the targeted hierarchical level of examination. Some studies focus on characteristics drawn from the entire population model (McDonald *et al.* 2017; Reed & Slade 2012). At this between-populations level (hereafter), a life history is considered demographically buffered if the governing demographic processes have low temporal variance (Le Coeur *et al.* 2022; Hilde *et al.* 2020; Morris & Doak 2004; Pfister 1998).

Deleted: achieving

Deleted: z

Deleted: ation

Deleted: '

Deleted: populations regarding demographic buffering

Deleted: typical

Deleted: (between-populations level)

Deleted: level

Deleted: key

However, to fully grasp how and why demographic buffering occurs, and how patterns might change in response to the environment, we must also consider characteristics within an individual population model (within-populations level hereafter). Within a population, one demographic process may be buffered against climatic variability while another may be labile (Barraquand & Yoccoz 2013; Jongejans *et al.* 2010; Koons *et al.* 2009). Furthermore, even if a given demographic process is primarily governing the population growth rate in one year, a different one might take over next year (Evers *et al.* 2021). Despite the relevance of within- and between-populations level processes, thus far studies have focused on evidencing

Deleted: at the level of separate components of

Deleted: the

Deleted: one

203 demographic buffering at the within- and between-population levels separately. To integrate  
204 these two levels of analysis, here we investigate demographic buffering signatures together.

205 To examine demographic buffering at the between-populations level, we use the  
206 summed effect of the variability of all demographic processes on the population growth rate.

207 A weak summed effect means that the population growth rate is relatively unaffected by the  
208 variability in demographic processes (Haridas & Tuljapurkar 2005), and this lack of effect by  
209 demographic process variability is consistent with demographic buffering. As such, a  
210 summed effect of variability offers a good proxy to evidence demographic buffering  
211 (Gascoigne *et al.* 2024b; Haridas & Tuljapurkar 2005) and enables the classification of  
212 populations along a continuum. The within-populations level requires a separate approach.

213 Thus, there we use the relative contribution of each demographic process and how variability  
214 in the governing demographic process(es) affects the population growth rate (*e.g.*, Caswell  
215 1978, 1996, 2001; Ebert 1999; de Kroon *et al.* 1986). Importantly, by exploring the governing  
216 demographic processes, we also investigate how natural selection affects them (*e.g.*, Caswell  
217 1996; Shyu & Caswell 2014). Understanding the interplay between demographic variability  
218 and natural selection thus not only elucidates population dynamics but also provides insight  
219 into the evolutionary pressures shaping the life-history strategies (Charlesworth 1994;  
220 Salguero-Gómez 2024; Sanghvi *et al.* 2024).

221 A powerful approach to reveal the role of natural selection acting on the variability of  
222 demographic processes is through measuring a first and second order effect on population  
223 growth rate (Carslake *et al.* 2008). First-order effects of demographic processes on population  
224 growth rate, such as elasticities, show how variation in demographic processes affects  
225 population growth rate, and relies on the linear relation between demographic processes and  
226 the growth rate. A second-order effect, on the other hand, reveals the sensitivity of population  
227 growth rate to temporal autocorrelation in variable environments (Tuljapurkar 1990), and

Deleted: focus

Deleted: o

Deleted: ' variability

Deleted: . Thus far, studies have focused on either one of the hierarchical levels, however, for a mechanistic understanding of how environmental stochasticity shapes life histories, both between- and within-population levels need to be addressed at the same time.

Deleted: here

Deleted: focus

Deleted: Namely, our interest was i

Deleted: o

Deleted: every

Deleted: ¶

Deleted: The complexity of examining the underlying mechanisms of demographic buffering presents additional challenge. Evidence suggests buffering in both long-lived , and short-lived species . However, these patterns alone do not fully reveal how life histories are shaped by natural selection. One useful way

Deleted: variance

Deleted: second-order

Deleted: of variation

identifies where demographic processes have a *nonlinear* effect on population growth rate. Combining both approaches into a single framework consolidates our understanding of fitness behaviour near local maxima and minima, among other advantages discussed below. This approach, and has started to pave its way into Ecology (Kajin *et al.* 2023; Tuljapurkar *et al.* 2023),

Here, we propose that an additional metric to examine demographic buffering: the second-order effect of demographic process variation on population growth rate. We show that each hierarchical level is best studied with a different method. Moreover, we hypothesise that buffered species, those where perturbing the variance of demographic processes has little impact on their fitness, are under strong concave selection pressures (*i.e.*, the force that aims to diminish temporal variance of a trait, sensu Shyu & Caswell 2014) on the governing demographic processes. Indeed, the summed effect of demographic process variability on population growth rate and elasticities are related (Haridas & Tuljapurkar 2005). Concave selection pressures favour traits that contribute to reducing temporal variance, thereby enhancing population stability and resilience in the face of environmental volatility. We discuss the validity of our hypothesis and demonstrate the applicability and advantages of our framework by testing it with 43 populations of 37 mammal species.

**Towards an integrated framework to assess evidence of demographic buffering**

Current evidence for demographic buffering has primarily been assessed using Matrix Population Models (MPMs) (Pfister 1998; Rotella *et al.* 2012). However, Integral Projection Models (IPMs) (Easterling *et al.* 2000; Ellner *et al.* 2016; Gascoigne *et al.* 2023a, 2024b; Rodríguez-Caro *et al.* 2021; Wang *et al.* 2023) can also identify demographic buffering. MPMs and IPMs are structured, discrete-time demographic models (Caswell 2001; Ellner *et al.* 2016). For simplicity, here we focus on MPMs, but the same approaches apply to IPMs

**Deleted:** A second-order effect can be measured by self-second derivatives of population growth rate with respect to every demographic process. While first-order effects on population growth rate, such as elasticities, show how variation in demographic processes affects population growth rate, while the second-order effects reveal sensitivity to autocorrelation. Integrating both approaches into a single framework enables an integrative allows a better understanding of fitness function behaviour near local maxima and minima

**Deleted:** -

**Deleted:** -

**Deleted:** finally

**Deleted:** c

**Deleted:** ¶  
In linear relationships between fitness and demographic processes, second-order derivatives of population growth rate (measuring a second-order effect on  $\lambda$ ) are zero, indicating natural selection acts on changing the mean values of demographic processes. Nonzero second derivatives suggest nonlinear relationships between fitness and a demographic process, revealing additional aspects of selection on the variances and covariances of demographic processes. Thus, it is of biological interest to join the information on first-order effect with the information on second-order effect. Furthermore, the sign ( $>0$ ,  $=0$ ,  $<0$ ) of the self-second derivative of  $\lambda$  with respect to demographic processes determines the type of selection. Negative values describe concave ( $\cap$ -shaped) selection, reducing temporal variance, providing information regarding the selection processes that might have led to an observed pattern of demographic

**Deleted:** - a

**Deleted:** - be added to the framework for evidencing ... [1]

**Deleted:** z

**Deleted:** integrated proposal

**Deleted:** applying

**Deleted:** to

**Deleted:** 0

**Deleted:** 4

**Deleted:** sourced from the COMADRE database (Salgado ... [3]

**Deleted:** Here, we introduce a framework to quantify ... [4]

**Deleted:** ). First, species or populations are positioned ... [5]

**Deleted:** . We showcase how the framework can provide ... [6]

**Deleted:** A

**Deleted:** unified

**Deleted:** framework

**Deleted:** The

**Deleted:** has been mainly assessed using Matrix Population Models ... [7]

**Deleted:**

**Deleted:** be equally applied for identifying signatures of ... [8]

**Deleted:**

**Deleted:** note that

**Deleted:** are as equally applicable

(Doak *et al.* 2021; Griffith 2017). We refer to demographic processes as MPM  $A$  entries  $a_{ij}$  (i.e., upper-level parameters *sensu* Zuidema & Franco 2001) and the vital rates composing the matrix elements (i.e., lower-level parameters, *ditto*). The conversion between matrix elements and vital rates is straightforward (Franco & Silvertown 2004).

We first place species on a variance continuum. The variance continuum represents the summed effects of proportional increases in temporal variance across all demographic processes ( $a_{ij}$ ) of the MPM  $A$  on the population growth rate  $\lambda_s$ , operating at the between-populations level. It is based on partitioning the sum of all the stochastic elasticities ( $\Sigma E_{a_{ij}}^S$ ) into two components: i) the sum of stochastic elasticities with respect to the variance ( $\Sigma E_{a_{ij}}^{S^\sigma}$ ), which assesses how variability in  $a_{ij}$  affects  $\lambda_s$ , and ii) the sum of stochastic elasticities with respect to the arithmetic mean of demographic processes ( $\Sigma E_{a_{ij}}^{S^\mu}$ ), which evaluates the impact of a change in mean values of demographic processes on  $\lambda_s$  (Haridas & Tuljapurkar 2005).

The equal perturbation of both  $\Sigma E_{a_{ij}}^S$  components assumes that the CV of demographic processes remains constant (Haridas & Tuljapurkar 2005). Higher absolute value of  $\Sigma E_{a_{ij}}^{S^\sigma}$  indicates greater sensitivity of  $\lambda_s$  to demographic process variability, suggesting the absence of demographic buffering. Conversely, lower  $\Sigma E_{a_{ij}}^{S^\sigma}$  values support the demographic buffering hypothesis, with  $\lambda_s$  being less sensitive to variability (Haridas & Tuljapurkar 2005; Tuljapurkar *et al.* 2003) (Fig. 1A).

Species or populations are positioned along the variance continuum based on the impact of variance on the stochastic population growth rate. Species highly sensitive to environmental variability are on the left (potentially unbuffered<sup>1</sup>), while species less sensitive

Deleted: Throughout this manuscript, w

Deleted: both

Deleted: matrix entries

Formatted: Font: Italic

Deleted: that underline

Deleted: , and note that their

Deleted: and described elsewhere

Deleted: The framework operates on three steps.

Deleted: In the first step of our framework, we

Deleted: start by

Deleted: calculating the impact of variation in demographic processes on the stochastic growth rate,  $\lambda_s$ , known as stochastic elasticities  $E_{ij}^S$  (Figure 1A). This calculation separates the sum of all stochastic elasticities into two components: one for assessing how temporal variance affects  $\lambda_s$  ( ), and the other for assessing the impact of mean values of demographic processes on  $\lambda_s$ , (

Deleted: A h

Deleted: the sum of stochastic elasticity with respect to variance (

Deleted: ),

Deleted: changes in

Deleted: demographic process variance

Deleted: e,

Deleted: ting

Deleted: a

Deleted: absolute value

Deleted: suggests

Deleted: where

Deleted: less

Deleted: such perturbations

Deleted:

Deleted: ¶

Deleted: Stochastic elasticities ( $E^S$ ) are calculated through equal perturbations to mean and variances in demographic processes across . This equal perturbation is an important assumption as the impacts of means and variances in demographic processes are inferred under the assumption that the coefficient of variation of said processes remains constant. Importantly, stochastic elasticities can be decomposed into contributions from means ( $\Sigma E_{a_{ij}}^{S^\mu}$ ) and variances ( $\Sigma E_{a_{ij}}^{S^\sigma}$ ) of demographic process.

Deleted: This

<sup>1</sup> Unconstrained variance does not necessarily imply demographic lability, defined as an increase in mean value of a demographic process in response to improved environmental conditions (Le Coeur *et al.* 2022). By examining stochastic elasticities, we can assess changes in the contribution of demographic process variance to  $\lambda_s$ , while mean values remain unchanged.



are on the right (potentially buffered) end (Fig. 1A). We expect buffered species to exhibit concave selection signatures. Although the position on the continuum provides insight into how environmental variation affects  $\lambda_s$ ,  $\Sigma E_{a_{ij}}^{\sigma}$  does not consider covariances between demographic processes and serial correlations, crucial for fully diagnosing buffering (Haridas & Tuljapurkar 2005). Thus, species' position at the buffered end of the variance continuum is a necessary but not sufficient condition for evidence of demographic buffering. To address this second criterion, we use second derivatives of population growth rate with respect to demographic processes to elucidate the impact of selection on variance (below).

Next, we delve into within-population level by calculating the partial derivatives of  $\lambda_t$  (obtained by averaging sequential MPMs across the study duration) concerning all matrix elements  $a_{ij}$  of the MPM  $A$  (Fig. 1B). This step reveals a first-order effect on fitness — how each demographic process influences  $\lambda_t$ . We then evaluate nonlinear selection patterns using self-second derivatives of  $\lambda_t$  for each  $a_{ij}$  (Fig. 1C), revealing potential nonlinear selection pressures (Brodie et al. 1995). Failure to consider these evolutionary processes may lead to misinterpretation of patterns (e.g., Lawler et al. 2009).

First- and second-order effects on fitness show average selection pressures over time. Self-second derivatives of population growth rate with respect to demographic processes measure second-order effects (Carslake et al. 2008; Caswell 2001; Kajin et al. 2023; Shyu & Caswell 2014; Tuljapurkar et al. 2023). Linear fitness relationships (zero self-second derivatives) mean selection changes mean demographic values, not variance (Shyu & Caswell 2014). Nonzero self-second derivatives indicate nonlinear relationships between fitness and a demographic process, revealing additional aspects of selection on the variances and covariances of demographic processes (Brodie et al. 1995; Carslake et al. 2008; Shyu & Caswell 2014). Interpreting both first- and second-order effects offers insights into population placement on the variance continuum.

**Deleted:** step places species or populations along a continuum based on variance in demographic processes, with unconstrained variance on the left (possibly unbuffered) and constrained variance on the right (possibly buffered)<sup>2</sup>

**Deleted:** .

**Deleted:** However, unconstrained variance does not necessarily imply demographic lability, defined as an increase in mean value of a demographic process in response to improved environmental conditions . By examining, we can assess changes in the contribution of demographic process variance to  $\lambda_s$ , while mean values remain unchanged.

**Deleted:** this step

**Deleted:** which are important

**Deleted:** Instead

**Deleted:** these

**Deleted:** a

**Deleted:** To address these criteria

**Deleted:** our approach focuses utilizeson

**Deleted:** selection's

**Deleted:** step 3,

**Deleted:** Steps 2 and 3 of the framework

**Deleted:** analyseis

**Deleted:** . After step 1 positions species or populations along the  $\Sigma E_{a_{ij}}^{\sigma}$  variance continuum for  $\lambda_s$ , each life cycle undergoes scrutiny. Step 2

**Deleted:** (Fig. 1B) involves calculating

**Deleted:**  $t$

**Deleted:**  $t$

**Deleted:** .

**Deleted:**  $t$

**Deleted:** In step 3

**Deleted:** , one

**Deleted:** s

**Deleted:**  $t$

**Deleted:** demographic process

**Deleted:** . This step unveils

**Deleted:** on demographic processes

**Deleted:** (Brodie et al. 1995)

**Deleted:** , crucial for understanding their evolutionary dynamics

**Deleted:** in step 1

**Deleted:** Lawler et al. 2009)

**Deleted:** )

**Deleted:** Steps 2 and 3

**Deleted:** of the framework analyse averaged selection pressures over time periods. They These steps offer insights into how perturbations in demographic processes affect  $\lambda_s$ , obtained by averaging sequential Matrix Population Models (MPMs) across the study duration. Therefore, they step (... [9]



558 The sign ( $>0$ ,  $=0$ ,  $<0$ ) of the self-second derivatives determines the selection type.  
559 Negative values (concave selection,  $\cap$ -shaped) reduce temporal variance, providing evidence  
560 of buffering (Caswell 1996, 2001; Shyu & Caswell 2014). Positive values (convex selection,  
561  $\cup$ -shaped) indicate amplified variance, revealing a lack of selection constraints on  
562 demographic variance (Bruijning *et al.* 2020; Caswell 1996, 2001; Le Coeur *et al.* 2022;  
563 Koons *et al.* 2009; Shyu & Caswell 2014; Vinton *et al.* 2022).

564 Following the above steps allows evidencing demographic buffering at the between-  
565 and within-populations levels. The joint interpretation of first- and second-order effects  
566 offers insights into why a population is on either end of the variance continuum. Evidence  
567 supporting buffering includes;

- 568 1. A population positioned near the 0 end of the  $\Sigma E_{a_{ij}}^{\sigma^2}$  continuum.
- 569 2. Identifying the demographic processes with highest elasticity values within the  
570 life cycle.
- 571 3. The same processes from (2) associated with negative self-second derivatives,  
572 indicating concave selection.

573 Figure 1B shows that, for an imaginary wolf population, the governing demographic process  
574 is the fourth stage stasis (MPM element  $a_{4,4}$ ), with the highest elasticity value (Fig. 1B yellow  
575 square). However, Figure 1C reveals little selection on  $a_{4,4}$  for variance reduction. Hence,  
576 there is no concave selection on  $a_{4,4}$ , explaining the positioning on the left-side variance  
577 continuum (Fig. 1A).

578 Although not our primary goal, we briefly introduce steps to evidence demographic  
579 lability. Compelling lability evidence requires sufficient data across environments [over time  
580 or space; but see Perret *et al.* (2024)] to construct reaction norms depicting demographic  
581 responses to environmental changes (Drake 2005; Koons *et al.* 2009; Morris *et al.* 2008).  
582 Non-linear relationships between demographic processes and the environment must be

**Deleted:** In step 3, it is important to note that the importance of demographic processes shifts with changing environments. This dynamic sensitivity of  $\lambda_t$  to specific processes, indicated by self-second derivatives, helps pinpoint which processes are most likely to induce changes in  $\lambda_t$ . For instance, in the hypothetical wolf species (Fig. 1), a decline in reproduction among third age-class individuals (matrix element  $a_{1,3}$ ) would heighten sensitivity to that process. Consequently, with increased environmental variability, the key demographic process might change from remaining in the fourth age class (matrix element  $a_{4,4}$ , Fig. 1B) to reproduction of the third age-class (matrix element  $a_{1,3}$ , Fig. 1C).  
Combining

**Deleted:** three

**Deleted:** of our framework

**Deleted:** a quantitative identification

**Deleted:** of

**Deleted:** Steps 2 and 3

**Deleted:** -- offer key insights as to why a given species or population is placed on either the buffered ( $\Sigma E_{a_{ij}}^{\sigma^2} \sim 0$ ) or the non-buffered end ( $\Sigma E_{a_{ij}}^{\sigma^2} \sim -1$ ) of the variance continuum. A clear and unequivocal evidence for support towards buffering consists of:

**Deleted:** (1)

**Deleted:** A species or population being positioned near the 0 end of the

**Deleted:** (the right-hand side) in step 1

**Deleted:** ; (2) this species' or populations' life cycle having one or more

**Deleted:** of population growth rate

**Deleted:** species' or populations'

**Deleted:** in step 2

**Deleted:** ;

**Deleted:** ¶

**Deleted:** the chosen

**Deleted:** of a hypothetical wolf species

**Deleted:** most important

**Deleted:** remaining in

**Deleted:** as this demographic process results in is associated

**Deleted:** .

**Deleted:** that  $a_{4,4}$  is under

**Deleted:** pressure

**Deleted:** Thus, there is no clear evidence of buffering (... [10])

**Deleted:** ).

**Deleted:** This way, the lack of concave selection force (... [11])

**Deleted:** here,

**Deleted:** said

**Deleted:** 4

**Deleted:** To establish compelling evidence of lability (... [12])

**Deleted:** However, we note that  $c$ , which can be chall (... [13])

established based on the reaction norms. Demographic processes where an increase in the mean value has a stronger positive impact on population growth rate than the detrimental effect of increased variance need to be identified. The latter condition is only met when the process-environment reaction norms are convex (Drake 2005, Koons *et al.* 2009, Morris *et al.* 2008) – but see Barraquand & Yoccoz (2013) for an alternative result. Importantly, species may not be purely buffered or labile some processes may be buffered, others labile, and others insensitive to environmental variability (e.g., Doak *et al.* 2005). Deciphering these patterns is a primary research interest in the field.

**Demographic buffering in mammals: A case study.**  
Here, we examine the performance of our framework and test our hypothesis, that is that species at the buffered end of the variance continuum display highly negative self-second derivatives for the governing demographic processes. We use 43 MPMs from 37 mammal species (16 species at the within-populations level). Mammals are of special interest in the context of demographic buffering for two reasons: (1) mammalian life histories have been well studied (Beccari *et al.* 2024; Bielby *et al.* 2007; Gillespie 1977; Jones 2011; Stearns 1983) and (2) some of their populations have already been assessed in terms of demographic buffering, particularly for primates (Campos *et al.* 2017; Morris *et al.* 2008, 2011; Reed & Slade 2012; Rotella *et al.* 2012). Together, the well-studied life histories and previous information about the occurrence of buffering in mammals allow us to make accurate predictions and validate the performance of our framework.

We used MPMs (Caswell 2001) from 43 out of 139 studies with mammals available in the COMADRE Animal Matrix Database v.3.0.0 (Salguero-Gómez *et al.* 2016). These 43 populations encompass 37 species from eight taxonomic orders. We carefully selected these MPMs in our analyses because their models contain values of demographic processes ( $a_{ij}$ )

Deleted: demographic process-environment

Deleted: Lastly, d

Deleted: s

Deleted: demographic

Deleted: takes a convex shape

Deleted: (resembling a "U" shape), as described by

Deleted: and

Deleted: . However, a study by

Deleted: reported

Deleted: diverging

Deleted: s in this regard

Deleted: demographically demographic processes

Deleted: Importantly, we note that more likely than previously thought (e.g., Pfister 1998), species do not exist as purely buffering or labile, but that within populations, some vital rates may be buffered, others labile, and others insensitive to the environment (e.g., (Doak *et al.* 2005). Deciphering generality in this likely complex pattern should attract much research attention going forward, in our opinion.

Deleted: using the unified framework

Deleted: W

Deleted: demonstrate

Deleted: framework

Deleted: integrated approach

Deleted: validate

Deleted: -

Deleted: using

Deleted: 44

Deleted: 34

Deleted: here

Deleted: provide the necessary information

Deleted: the proposed

Deleted: Matrix Population Models (

Deleted:

Deleted: ,

Deleted: 0

Deleted: d

Deleted:

Deleted: 0

Deleted: 4

Deleted: included

Deleted: ,

Deleted: y

Deleted: provide

for three or more contiguous time periods, thus allowing us to obtain the stochastic elasticity of each  $a_{ij}$ . Although we are aware that not all possible temporal variation in demographic processes may have been expressed within this period, we assumed three or more transitions are enough to provide sufficient variation for population comparison (Compagnoni *et al.* 2023). To mitigate bias in variance estimates, we randomly extracted three MPMs from the existing data for each species (Supplementary Material, Table S1), calculated the mean of these three MPMs, and repeated this process 50 times to obtain estimates of  $\Sigma E_{a_{ij}}^{S\sigma}$  and their corresponding standard errors. A detailed description of the analysed data and their original sources are detailed in Table S1. Finally, we included MPMs of *Homo sapiens* to cross-check our estimates of second-order derivatives, as it is the only mammalian species where these have been calculated (Caswell 1996). The data for *H. sapiens* were gathered from 26 modern populations (Keyfitz & Flieger 1990).

At the within-populations level, we used a subset of 16 populations (including *H. sapiens*) whose MPMs were age-based. We specifically selected these populations because their life cycles can be summarised by two main demographic processes: survival and contribution to the recruitment of new individuals (Caswell 2010; Ebert 1999).

To quantify the variance continuum and calculate  $\Sigma E_{a_{ij}}^{S\sigma}$  for between-populations level comparisons, we followed Tuljapurkar *et al.* (2003) and Haridas & Tuljapurkar (2005). Next, at the within-populations level, we calculated the deterministic elasticities to each demographic process using the *popbio* package (Stubben *et al.* 2020). The self-second derivatives were adapted from *demogR* (Jones 2007) following (Caswell 1996) and applied to the mean MPM of each study. All analyses were performed using R version 4.4.1 (R Core Team 2024).

## Results

Deleted:

Deleted: matrices

Deleted: number of matrices detailed in

Deleted: matrices

Deleted: Fortunately, several long-lived species, characterized by low variation in their demographic processes, were studied for a long time (e.g., some primates in our dataset have been studied for over 20 years – Morris *et al.* 2011). We removed the populations where either only survival or only reproduction rates were reported, because of the impossibility to calculate the stochastic growth rate.

Deleted: available in supplementary material (Supple... [14])

Deleted: )

Deleted: ¶

Deleted: as a way

Deleted: was included in our analyses because

Deleted: before

Deleted: in which second-order derivatives have been applied

Deleted: Therefore, *Homo sapiens* provides an ideal b... [15]

Deleted: omo

Deleted: located in various cities, allowing us to const... [16]

Deleted: For steps 2 and 3 of our framework,

Deleted: utilized

Deleted: *Homo*

Deleted: population projection matrices (

Deleted: )

Deleted: organized by

Deleted: z

Deleted: .

Deleted: The contribution to recruitment can be inter... [17]

Deleted: One advantage of using such matrices MPM... [18]

Deleted: perform the step 1 of our framework

Deleted: obtain

Deleted: the

Deleted: (and  $\Sigma E_{a_{ij}}^{S\sigma}$ )

Deleted: (

Deleted: (

Deleted: To perform step 2 of our framework

Deleted: -

Deleted: -

Deleted: ,

Deleted: of

Deleted: extracted

Deleted: All analyses were performed using R version... [19]

Deleted: to perform the step 3 of our framework t

Deleted: for

807 We ranked 43 populations from the 37 identified mammal species into a variance continuum  
808 according to the cumulative impact of variation in demographic processes on  $\lambda_s$  (Fig. 2). Most  
809 of the analysed taxonomic orders were placed on the low or zero variance end of the variance  
810 continuum (Fig. 2), corroborating with demographically buffered populations. The smallest  
811 contributions of variation in demographic processes (note that  $\Sigma E_{a_{ij}}^{S\sigma}$  ranges from 0 to -1),  
812 suggesting buffered populations, were assigned to Primates: northern muriqui (*Brachyteles*  
813 *hyphoxantus*,  $\Sigma E_{a_{ij}}^{S\sigma} = -5.31 \times 10^{-5} \pm 2.09 \times 10^{-5}$ ) (mean  $\pm$  S.E.) (Fig. 2 silhouette a), mountain  
814 gorilla (*Gorilla beringei*,  $\Sigma E_{a_{ij}}^{S\sigma} = -1.28 \times 10^{-5} \pm 1.32 \times 10^{-5}$ ) (Fig. 2 silhouette b), followed by  
815 the blue monkey (*Cercopithecus mitis*,  $\Sigma E_{a_{ij}}^{S\sigma} = -4.43 \times 10^{-5} \pm 1.18 \times 10^{-5}$ ) (Fig. 2 silhouette  
816 c). The first non-primate species placed near the buffered end of the continuum was the  
817 Columbian ground squirrel (*Uroditellus columbianus*, Rodentia,  $\Sigma E_{a_{ij}}^{S\sigma} = -3.38 \times 10^{-3} \pm 6.96 \times$   
818  $10^{-4}$ ) (Fig. 2 silhouette d). On the other opposite, the species with the highest contribution of  
819 variation in demographic processes  $\rightarrow$  placed at the high-variance end of the continuum  $\rightarrow$   
820 was the stoat (*Mustela erminea*, Carnivora,  $\Sigma E_{a_{ij}}^{S\sigma} = -0.310 \pm 0.0162$ ) (Fig. 2 silhouette e). All  
821 the 14 primate populations occupied the buffered side of the variance continuum, with the  
822 exception of the Patas monkey (*Erythrocebus patas*, Primates,  $\Sigma E_{a_{ij}}^{S\sigma} = -0.0521 \pm 5.38 \times 10^{-3}$ )  
823 (Fig. 2 silhouette f). The snowshoe hare (*Lepus americanus*, Lagomorpha,  $\Sigma E_{a_{ij}}^{S\sigma} = -0.262 \pm$   
824  $0.0233$ ) (Fig. 2 silhouette g) and the Bush rat (*Rattus fuscipes*, Rodentia,  $\Sigma E_{a_{ij}}^{S\sigma} = -0.245 \pm$   
825  $4.29 \times 10^{-3}$ ) (Fig. 2 silhouette h) were positioned on the non-buffered end of the variance  
826 continuum. Additional information (including standard errors of the elasticity estimates) is  
827 provided in Table S1. A posteriori, we quantified the impact of phylogenetic relatedness on  
828 the estimates of the sum of stochastic elasticities (Fig. 2), and then for the correlation  
829 between those estimates and the number of MPMs available per species. For the former, we  
830 estimated Blomberg's K, a measure of phylogenetic signal that ranges between 0 (weak

Deleted: 40 ...opulations from the 37 34 (... [20])

Deleted: using the step 1 of our framework ... Fig. 2). Additional information (including standard deviations of the deviations of the elasticity estimates and number of matrices available) is provided in the supplementary material (Table S1). ...ost of the analysed taxonomic orders were placed on the low-... or zero variance end of the variance continuum 2), corroborating with demographically...emographically buffered populations. The smallest contributions of variation in demographic processes (i.e., maximum value o, (... [21])

Deleted: more

Deleted:  $0.09... \times 10^{-54} ... \pm 2.090.12... \times 10^{-54}$  (... [22])

Deleted: standard ...E.error (... [23])

Deleted: deviation

Deleted: h

Deleted:  $0.24... \times 10^{-54} ... \pm 1.320.08... \times 10^{-54}$  (... [24])

Deleted:  $0.63... \times 10^{-54} ... \pm 1.180.06... \times 10^{-54}$  (... [25])

Deleted: low-variance

Deleted:  $-0.003...3.38 \times 10^{-3} \pm 6.96 -4.430.63... \times 10^{-4}$  (... [26])

Deleted: T

Deleted: -... placed at the high-variance end of the continuum  $\rightarrow$  (... [27])

Deleted:  $5... \pm 0.01622$  (... [28])

Deleted: displayed potential evidence of buffering, occupying...the right-hand (... [29])

Deleted: 0.03

Deleted:  $9... \pm 0.023316$  (... [30])

Deleted: 0.03

Deleted: appear ...ere positioned on the high-variance (... [31])

Deleted: the Supplementary material (...able S1)... A posteriori, we tested...uantified for (... [32])

Deleted: strength...mpact of phylogenetic relatedness on the estimates of the sum of stochastic elasticities (Fig. 2), and then for the correlation between those estimates and the number of MPMs available per species. For the former, we estimated Blomberg's K, (...n...estimate (... [33])

Deleted: [

937 signal) to positive values 1 (strong) (Münkemüller *et al.* 2012). Blomberg's K in our analyses  
 938 was 0.23. The correlation between the number of available MPMs per study and the sum of  
 939 stochastic elasticities (post jack-knifing) raised a weakly negative coefficient (-0.002), though  
 940 significant ( $P = 0.017$ ).

941 We found little evidence in support of our hypothesis. Specifically, the demographic  
 942 processes with the highest elasticity values failed to display strong negative self-second  
 943 derivatives (Fig. 3). Particularly for the majority of primates, demographic processes with  
 944 high elasticities had positive values for the self-second derivatives (indicated by yellow  
 945 squares with white dots in Figure 3). Examples of primate species exhibiting high elasticities  
 946 and positive values for their self-second derivatives include northern muriqui (*Brachyteles*  
 947 *hypoxanthus*), mountain gorilla (*Gorilla beringei*), white-faced capuchin monkey (*Cebus*  
 948 *capucinus*), rhesus monkey (*Macaca mulatta*), blue monkey (*Cercopithecus mitis*),  
 949 Verreaux's sifaka (*Propithecus verreauxi*) and olive baboon (*Papio cynocephalus*) (Fig. 3).

950 This implies that the key demographic processes influencing  $\lambda_i$  do not show evidence of  
 951 selective pressure for reducing their variability.

952 The killer whale (*Orcinus orca*) showed similar lack of support for our hypothesis as  
 953 primates. Indeed, *O. orca* was positioned at the buffered end of the variance continuum  
 954 (Cetacea,  $\Sigma E_{a_{ij}}^{S\sigma} = -4.72 \times 10^{-4} \pm 1.53 \times 10^{-4}$ ) (Fig. 2 silhouette not shown). However, the first-  
 955 and second-order effects show that the governing three demographic processes in the killer  
 956 whale life cycle (namely, matrix elements  $a_{2,2}$ ,  $a_{3,3}$ , and  $a_{4,4}$ ) are not under selection pressures  
 957 for reducing their temporal variance, but the opposite (yellow and green squares with white  
 958 dots, Fig. 3).

959 Only two species supported our hypothesis: humans and the Columbian ground  
 960 squirrel (*Urocyon columbianus*). In humans, demographic parameters representing survival  
 961 from the first to second age class (matrix element  $a_{2,1}$ ) displayed high elasticities and negative

Deleted: even

Deleted:

Deleted: As predicted for the steps 2 and 3,

Deleted: w

Deleted: could not observe a clear pattern in support of buffering

Deleted: Indeed

Deleted: This finding means that

Deleted: ly

Deleted: - with the a lack or minor temporal variation in demographic processes -

Deleted: .

Deleted: and

Deleted: ,

Deleted: are

Deleted: not subject to

Deleted: temporal

Deleted: However, even though the primates were positioned closer to the low-variance end of the continuum in step 1, the evidence from steps 2 and 3 does not support the occurrence of buffering in the most influential demographic processes.

Deleted: controversy between the results of step 1 and steps 2-3 results as most primates. In step 1, t

Deleted: The

Deleted: killer whale

Formatted: Font: Italic

Deleted: *Orcinus orca*,

Deleted: 0.70

Deleted: 04

Deleted: <sup>5</sup>

Deleted: steps 2 and 3

Deleted:

Deleted: with highest elasticity values

Deleted:

Deleted: depicted by

Deleted: The only primate species exhibiting evidence of buffering in steps 2 and 3 corroborating our hypothesis was the human

self-second derivatives (depicted as yellow squares with black dots in Fig. 3). In *U. columbianus*, survival from the first to the second age class ( $a_{2,1}$ ) too showed evidence of selection reducing the variance of this demographic process. Accordingly, *U. columbianus* was positioned near the buffered end of the variance continuum, providing consistent evidence supporting our hypothesis by displaying first- and second-order effects indicative of temporal variance reduction in the key demographic process. Conversely, the primary governing demographic process for Soay sheep (*Ovis aries*) displayed convex selection signatures. For *O. aries* (Fig. 2, silhouette i), remaining in the third age class ( $a_{3,3}$ , Fig. 3) governs the influence on  $\lambda_t$  and is under selection pressure to have its variance increased. These characteristics suggest potential conditions for lability, despite the species being positioned closer to the buffered end of the variance continuum.

The first- and second-order effects illustrate the importance of examining buffering evidence at the within-populations level. These effects can identify the simultaneous contributions of concave and convex selection on different demographic processes within a single life cycle. In the polar bear (*Ursus maritimus*), the key demographic process ( $a_{4,4}$ ) is under convex selection, as depicted by a yellow square with a white dot in Figure 3. However, the demographic process with the second highest elasticity value ( $a_{5,4}$ ) is under strong concave selection (depicted by a light green square with a black dot in Figure 3).

By adding the second-order effect to the toolbox for demographic buffering, another important inference was made possible. The high absolute values of self-second derivatives (large dots, either black or white, Fig. 3) indicate where the sensitivity of  $\lambda_t$  to demographic parameters is itself prone to environmental changes. For instance, if the value of  $a_{5,4}$  for *U. maritimus* increased, the sensitivity of  $\lambda_t$  to  $a_{5,4}$  would decrease because the self-second derivative of  $a_{5,4}$  is highly negative (depicted by the largest black dot in polar bear, Fig. 3 silhouette i). The opposite holds for the  $a_{4,4}$  demographic process, where an increase in the

Deleted: Evidence supporting buffering our hypothesis was also found in the Columbian ground squirrel

Deleted: (*Urocitellus columbianus*), where, similar tolkie in humans

Deleted: matrix element

Deleted: indications

Deleted: acting to reduce

Deleted:  $a_{2,1}$  variance

Deleted: the Columbian ground squirrel

Deleted: was positioned close to the buffered end of the variance continuum in step 1. Hence, this speciese Columbian ground squirrel was the sole species was the only one with consistent evidence of buffering -- across all three steps of the framework.

Deleted: ¶

Deleted: The Soay sheep (*Ovis aries*) was the species furthest from the buffered end of the variance continuum that enabled to perform steps 2 and 3.

Deleted: the Soay sheep

Deleted: matrix element

Deleted: has

Deleted: major

Deleted: The latter characteristics reveal potential conditions for lability even though the species is placed closer to the buffered end of the variance continuum. ¶

Deleted: Steps 2 and 3

Deleted:

Deleted: on

Deleted: two steps of the framework

Deleted: acting

Deleted: s

Deleted: matrix element

Deleted: .

Deleted: matrix element

Deleted: step 3

Deleted: framework

Deleted: information

Deleted: was accessed

Deleted:  $\lambda_t$

Deleted: polar bear

Deleted:

Deleted: MPM

Deleted: Vice versa



value of  $a_{4,4}$  would increase the sensitivity of  $\lambda_4$  to  $a_{4,4}$ , because the self-second derivative of  $a_{4,4}$  is highly positive (the largest white dot in the polar bear MPM). Thus, sensitivities (or equally elasticities) of demographic processes with high absolute values for self-second derivatives are dynamic and can easily change.

Deleted: 's sensitivity

Deleted: <sub>5</sub>

Deleted: depicted by

Deleted: can

## Discussion

We report evidence of demographic buffering assessed at the between and within populations level. We used stochastic elasticities alongside the first- and second- order perturbation analysis and applied these analyses to mammal species to test our hypothesis. Here, we find weak support for said hypothesis, since most populations placed at the buffered end of variance continuum failed to display concave selection signatures.

Evidencing demographic buffering is not straightforward. Indeed, through the analysis of stochastic population growth rate ( $\lambda_s$ ) in our application of the framework to 43 populations of 37 mammal species, we identify the highest density of natural populations near the buffered end of the variance continuum. However, we show that the same species then fail to exhibit signs of concave ( $\cap$ -shaped) selection on key demographic parameters. Such results suggest discordance between two features of demographic buffering, namely: 1) the stochastic population growth rate having a low sensitivity to temporal variability in demographic processes, and 2) demographic processes having variability constrained by selection.

Deleted: In the Anthropocene, identifying and quantifying mechanisms of species responses to stochastic environments holds crucial importance. This importance is particularly tangible in the context of the unprecedented environmental changes and uncertainties that impact the dynamics and persistence of natural populations. Correlational demographic analysis, whereby the importance of demographic processes and their temporal variability is examined, has attempted to identify how species may buffer against the negative effects of environmental stochasticity. However, these widely used approaches have important limitations (see Introduction and Hilde *et al.* 2020). One significant limitation is the issue of measurement scale concerning demographic processes. Demographic processes, such as birth rates, death rates, immigration, and emigration, operate at various temporal and spatial scales. The choice of scale at which these processes are measured can impact the outcomes of correlational demographic analysis. Our novel framework overcomes said limitations by providing a rigorous approach to quantify demographic buffering (.

Deleted: 44

Deleted: 34

Deleted: (step 1)

Deleted: the

Deleted:

Deleted: when further analyses are performed averaging the variation across the duration of each study (steps 2 and 3)

Deleted: This

The lack of correlation between non-linear selection patterns (concave/convex) and species positioning on the variance continuum for the studied mammal species may have several explanations. Firstly, non-linear selection on demographic process variability is dynamic (Kajin *et al.* 2023). Within a life cycle, even minor changes in key demographic processes can trigger a domino effect, affecting not only the process itself but also the



sensitivity of  $\lambda_1$  to changes in said process (Stearns 1992). Consequently, correlations between demographic processes (negative correlations known as trade-offs) are influenced by minor alterations in the governing demographic processes (Doak *et al.* 2005). Therefore, the observed self-second derivative of the population growth rate represents a momentum that can be influenced by small changes in any demographic process within the life cycle. Because of these characteristics, second-order derivatives reveal “fine scale” fitness behaviour compared to sums of stochastic elasticities. Evolutionary demography still requires a tool to connect second-order fitness effects with stochastic elasticities in a biologically interpretable manner (but see Tuljapurkar *et al.* 2023).

When placing our study species along a variance continuum, primates tend to be located on the buffered end. However, most primates displayed convex – instead of the expected concave – selection on adult survival. Similar results, where the key demographic process failed to display constrained temporal variability, have been reported for long-lived seabirds (Doherty *et al.* 2004). One explanation for the unexpected convex selection on adult survival involves trade-offs, as suggested by (Doak *et al.* 2005). When two demographic parameters are negatively correlated, the variance of population growth rate can be increased or decreased (Compagnoni *et al.* 2016; Evans & Holsinger 2012).

Correlations among demographic processes (positive and negative) inherently influence the biological limits of variance (Haridas & Tuljapurkar 2005). This is because the magnitude of variation in a particular demographic process is constrained by the variation of other demographic processes. Not surprisingly, correlations among demographic processes have been shown to be strongly subjected to ecological factors (Fay *et al.* 2022). Therefore, future studies may benefit from deeper insights using cross-second derivatives (Caswell 1996, 2001) to investigate correlations among demographic processes.

**Deleted:** finding confirms that placing the species near the buffered end of the variance continuum is *necessary* but not *sufficient* to diagnose demographic buffering. Indeed, buffering occurs when concave selection forces act on the key demographic parameter . ¶

Biological variance estimates are inevitably subjected to several sources of bias (Simmonds & Jones 2024). To minimise bias, we randomly sampled the available matrices before obtaining the estimates. Despite the significant correlation between  $\Sigma E_{a_{ij}}^{S\sigma}$  and the number of available matrices per species, the relative positioning of species remains meaningful for between-population level comparisons, as the correlation is very weak (-0.002). Still, researchers carrying out macroecological comparisons of demographic buffering might want to be even more restraining than we have been here with their datasets, as these grow longer with time (Compagnoni *et al.* 2021; Salguero-Gómez *et al.* 2021).

Regarding phylogenetic effects, our tests revealed a mild signal, but we note that future work regressing  $\Sigma E_{a_{ij}}^{S\sigma}$  values against potential independent variables (*e.g.*, climate values) may want to correct for this phylogenetic dependence. By having carefully chosen studies from a database that contains >400 species and retained only those that passed through a set of selection criteria (Che-Castaldo *et al.* 2020; Gascoigne *et al.* 2023b; Kendall *et al.* 2019; Römer *et al.* 2024; Simmonds & Jones 2024), we mitigate those biases *a priori*. Furthermore, we are using an elasticity-based approach, meaning we are comparing proportional variances. At present, the available methods still do not account for constraints in variance nor performing a perturbation approach disproportionately.

The analyses at both between- and within-populations levels are fundamentally interconnected. This connection is grounded on the fact that large summed elasticities with respect to variance are intrinsically linked to high elasticity values, as demonstrated in equation 6 in (Haridas & Tuljapurkar 2005). This finding robustly endorses the perspective that species' positions along the variance continuum should be interpreted with consideration of first and second-order effects, and additionally, in the context of selection pressures acting on the variability of demographic processes, as revealed by a second order effect.

Combining first- and second-order analyses is crucial for understanding the factors shaping demographic buffering patterns. The second-order effect reveals that the role of natural selection in shaping temporal variation in demographic processes is more complex than initially thought. Indeed, demographic processes within our study populations often face a mix of convex and concave selection. This mix of selection patterns was suggested by Doak et al. (2005), who noted that dramatic changes in population growth rate sensitivities are influenced by correlations among demographic processes. Here, only two of the 16 mammal species revealed concave selection on the key demographic processes: Colombian ground squirrel (*Uroditellus columbianus*), and humans, (*Homo sapiens*). These two species were placed near the buffered end of the variance continuum, supporting our hypothesis. Evidence of buffering has been reported across 22 ungulate species (Gaillard & Yoccoz 2003). However, in the one ungulate we examined, the moose (*Alces alces*), we found only partial support for our hypothesis, as it is near the buffered end of the variance continuum but lacks concave selection pressures.

Our overall findings reveal varying levels of support for the notion that adult survival in long-lived species tends to be buffered. Indeed, Gaillard et al. (1998) found that adult female survival varied considerably less than juvenile survival in large herbivores. This finding was also supported by further studies in ungulates (Gaillard & Yoccoz 2003), turtles (Heppell 1998), vertebrates and plants (Pfister 1998), and more recently across nine species of plants (McDonald et al. 2017). However, an alternative result was also reported by Gaillard and Yoccoz (2003) for small mammals, where variability in adult survival was unexpectedly high, even though the studied small mammals were annual, and as such comparable to large mammal model. Seasonality, frequency and method of sampling all influence survival estimates and their estimated variability, thus, when comparing multiples

**Deleted:** Combining the three steps into a unified framework is of utmost importance. In steps 2 and 3 of the framework, we find relatively limited overall evidence of buffering in the examination of our 16 (out of 34 in step 1) studied animal species (out of 34 in step 1). Step 3 of our framework reveals that the role of natural selection shaping temporal variation in demographic processes is more complex than expected. Indeed, demographic processes within our study populations are often under a mix of convex and concave selection. This mix of selection patterns was already suggested by Doak et al. (2005).

**Deleted:** out

**Deleted:** acting

**Deleted:** (Colombian ground squirrel [*Uroditellus columbianus*], and humans, [*Homo sapiens sapiens*])

**Deleted:** also

**Deleted:** therefore

**Deleted:** meeting all the necessary conditions to diagnose buffering

**Deleted:** However, finding 12.5% (two out of 16) species that meet the criteria for demographic buffering is not in concordance with previous studies.

**Deleted:** I

**Deleted:** find

**Deleted:** buffering in adult survival

**Deleted:** since this species is placed

**Deleted:** in step 1

**Deleted:** does not show

**Deleted:** on adult survival in step 2/3, as would be necessary to confirm the occurrence of buffering

**Deleted:** It is worth noting that a varying number of matrices per species were employed, ranging from 1 to 21, with an average of 8.1 matrices per species (as shown in Table S1). Naturally, having a greater number of matrices is preferred in such analyses. Furthermore, while the size of matrices (matrix dimensions) does not directly bias the results of our framework in any way – since steps 2 and 3 are shown for all the demographic processes independent of matrix dimension – potential implications of varying matrix dimensions should be further investigated in the future. ¶

1242 [species/studies, all of the latter characteristics should be taken into account when interpreting](#)  
1243 [the results.](#)

1244 [Examining the drivers of demographic buffering has become an important piece of the](#)  
1245 ecological and evolutionary puzzle of demography. As such, [understanding](#) buffering can  
1246 help us better predict population responses to environmental variability, climate change, and  
1247 direct anthropogenic disturbances ([Boyce et al. 2006; Gascoigne et al. 2024a; McDonald et](#)  
1248 [al. 2017; Pfister 1998; Vázquez et al. 2017](#)). By setting demographic buffering into a broader  
1249 and integrated framework, we hope to enhance comprehension and prediction of the  
1250 implications of heightened environmental stochasticity on the evolution of life history traits.  
1251 This understanding is crucial in mitigating the risk of extinction for the most vulnerable  
1252 species.

## 1253 [▼](#)

### 1254 Acknowledgements

1255 This study was financed in part by the *Coordenação de Aperfeiçoamento de Pessoal de Nível*  
1256 *Superior* - Brasil (CAPES) - Finance Code 001. GSS was supported by CAPES and CNPq  
1257 (301343/2023-3). [MK was supported by the European Commission through the Marie](#)  
1258 [Sklódowska-Curie fellowship \(MSCA MaxPersist #101032484\) hosted by RSG.](#)  
1259 RS-G was supported by a NERC Independent Research Fellowship (NE/M018458/1) [and a](#)  
1260 [NERC Pushing the Frontiers \(NE/X013766/1\).](#) ▲

### 1261

### 1262 Data availability

1263 The demographic data used in this paper are open-access and available in the COMADRE  
1264 Animal Matrix Database (<https://compadre-db.org/Data/Comadre>). A list of the studies and  
1265 species used here is available in Supplementary Material (Table S1). The data and code

**Deleted:** When placing our study species along a variance continuum (step 1), primates tend to be located on the buffered end. However, most primates displayed convex – instead of the expected concave– selection on adult survival. Similar results, where the key demographic process failed to display constrained temporal variability, have been reported for long-lived seabirds . One explanation for the unexpected convex selection on adult survival involves trade-offs, as suggested by . When two demographic parameters are negatively correlated, the variance of population growth rate ( $\lambda$ ) can be increased or decreased . The well-established trade-off between survival and fecundity might explain the observed deviation of our results. Because variation in primate recruitment is already constrained by physiological limitations , when adult survival and recruitment are engaged in a trade-off, this trade-off might lead to our unexpected result. Correlations among demographic processes (positive and negative) inherently influence the biological limits of variance (Haridas & Tuljapurkar, 2005). This is because the magnitude of variation in a particular demographic process is constrained by (the variation of) other demographic processes that exert an influence on it. Not surprisingly, correlations among demographic processes have been shown to be strongly subjected to ecological factors . Here Therefore, future studies may benefit from deeper insights via using cross-second derivatives to investigate correlations among demographic processes. ¶

**Deleted:** quantifying

**Deleted:** In the Anthropocene, identifying and quantifying mechanisms of species responses to stochastic environments holds crucial importance. This importance is particularly tangible in the context of the unprecedented environmental changes and uncertainties that impact the dynamics and persistence of natural populations . Correlational demographic analysis, whereby the importance of demographic processes and their temporal variability is examined , has attempted to identify how species may buffer against the negative effects of environmental stochasticity. However, these widely used approaches have important limitations (see Introduction and Hilde et al. 2020). One significant limitation is the issue of measurement scale concerning demographic processes . Demographic processes, such as birth rates, death rates, immigration, and emigration, operate at various temporal and spatial scales. The choice of scale at which these processes are measured can impact the outcomes of correlational demographic analysis . Our novel framework overcomes said limitations by providing a rigorous approach to quantify demographic buffering (. ¶

**Moved (insertion) [1]**

**Moved up [1]:** MK was supported by the European Commission through the Marie Skłodowska-Curie fellowship (MSCA MaxPersist #101032484) hosted by RSG.

1318 supporting the results can be accessed here:

1319 [https://github.com/SamuelGascoigne/Demographic\\_buffering\\_unified\\_framework](https://github.com/SamuelGascoigne/Demographic_buffering_unified_framework).

1320

## 1321 References

- 1322 [Barraquand, F. & Yoccoz, N.G. \(2013\). When can environmental variability benefit](#)  
1323 [population growth? Counterintuitive effects of nonlinearities in vital rates. \*Theor Popul\*](#)  
1324 [Biol, 89, 1–11.](#)
- 1325 [Bathiany, S., Dakos, V., Scheffer, M. & Lenton, T.M. \(2018\). Climate models predict](#)  
1326 [increasing temperature variability in poor countries. \*Sci Adv\*, 4.](#)
- 1327 [Beccari, E., Capdevila, P., Salguero-Gómez, R. & Carmona, C.P. \(2024\). Worldwide](#)  
1328 [diversity in mammalian life histories: Environmental realms and evolutionary](#)  
1329 [adaptations. \*Ecol Lett\*, 27.](#)
- 1330 [Bielby, J., Mace, G.M., Bininda-Emonds, O.R.P., Cardillo, M., Gittleman, J.L., Jones, K.E.,](#)  
1331 [et al. \(2007\). The Fast-Slow Continuum in Mammalian Life History: An Empirical](#)  
1332 [Reevaluation. \*Am Nat\*, 169, 748–757.](#)
- 1333 [Bonsall, M.B. & Klug, H. \(2011\). The evolution of parental care in stochastic environments.](#)  
1334 [J Evol Biol, 24, 645–655.](#)
- 1335 [Boyce, M., Haridas, C., Lee, C. & The NCEAS Stochastic Demography Working Group.](#)  
1336 [\(2006\). Demography in an increasingly variable world. \*Trends Ecol Evol\*, 21, 141–148.](#)
- 1337 [Brodie, E.I., Moore, A. & Janzen, F. \(1995\). Visualizing and quantifying natural selection.](#)  
1338 [Trends Ecol Evol, 10, 313–318.](#)
- 1339 [Campos, F.A., Morris, W.F., Alberts, S.C., Altmann, J., Brockman, D.K., Cords, M., et al.](#)  
1340 [\(2017\). Does climate variability influence the demography of wild primates? Evidence](#)  
1341 [from long-term life-history data in seven species. \*Glob Chang Biol\*, 23, 4907–4921.](#)
- 1342 [Carslake, D., Townley, S. & Hodgson, D.J. \(2008\). Nonlinearity in eigenvalue-perturbation](#)  
1343 [curves of simulated population projection matrices. \*Theor Popul Biol\*, 73, 498–505.](#)
- 1344 [Caswell, H. \(1978\). A general formula for the sensitivity of population growth rate to](#)  
1345 [changes in life history parameters. \*Theor Popul Biol\*, 14, 215–230.](#)
- 1346 [Caswell, H. \(1996\). Second Derivatives of Population Growth Rate: Calculation and](#)  
1347 [Applications. \*Ecology\*, 77, 870–879.](#)
- 1348 [Caswell, H. \(2001\). \*Matrix Population Models: Construction, Analysis, and Interpretation\*.](#)  
1349 [Sinauer Associates Inc. Publishers, Sunderland, Massachusetts, USA.](#)
- 1350 [Charlesworth, B. \(1994\). \*Evolution in age-structured populations\*. second edi. Cambridge](#)  
1351 [University Press.](#)
- 1352 [Che-Castaldo, J., Jones, O.R., Kendall, B.E., Burns, J.H., Childs, D.Z., Ezard, T.H.G., et al.](#)  
1353 [\(2020\). Comments to “Persistent problems in the construction of matrix population](#)  
1354 [models.” \*Ecol Modell\*, 416.](#)
- 1355 [Le Coeur, C., Yoccoz, N.G., Salguero-Gómez, R. & Vindenes, Y. \(2022\). Life history](#)  
1356 [adaptations to fluctuating environments: Combined effects of demographic buffering](#)  
1357 [and lability. \*Ecol Lett\*, 25, 2107–2119.](#)
- 1358 [Compagnoni, A., Bibian, A.J., Ochocki, B.M., Rogers, H.S., Schultz, E.L., Sneek, M.E., et](#)  
1359 [al. \(2016\). The effect of demographic correlations on the stochastic population dynamics](#)  
1360 [of perennial plants. \*Ecol Monogr\*, 86, 480–494.](#)
- 1361 [Compagnoni, A., Evers, S. & Knight, T. \(2023\). Spatial replication can best advance our](#)  
1362 [understanding of population responses to climate. \*bioRxiv\*,](#)  
1363 <https://doi.org/10.1101/2022.06.24.497542>.

Compagnoni, A., Levin, S., Childs, D.Z., Harpole, S., Paniw, M., Römer, G., *et al.* (2021). Herbaceous perennial plants with short generation time have stronger responses to climate anomalies than those with longer generation time. *Nat Commun*, 12, 1824.

Doak, D.F., Morris, W.F., Pfister, C., Kendall, B.E. & Bruna, E.M. (2005). Correctly Estimating How Environmental Stochasticity Influences Fitness and Population Growth. *Am Nat*, 166, E14–E21.

Doak, D.F., Waddle, E., Langendorf, R.E., Louthan, A.M., Isabelle Chardon, N., Dibner, R.R., *et al.* (2021). A critical comparison of integral projection and matrix projection models for demographic analysis. *Ecol Monogr*, 91, e01447.

Doherty, P.F., Schreiber, E.A., Nichols, J.D., Hines, J.E., Link, W.A., Schenk, G.A., *et al.* (2004). Testing life history predictions in a long-lived seabird: A population matrix approach with improved parameter estimation. *Oikos*, 105, 606–618.

Drake, J.M. (2005). Population effects of increased climate variation. *Proceedings of the Royal Society B: Biological Sciences*, 272, 1823–1827.

Easterling, M.R., Ellner, S.P. & Dixon, P.M. (2000). Size-Specific Sensitivity: Applying a New Structured Population Model. *Ecology*, 81, 694–708.

Ebert, T. (1999). *Plant and animal populations: Methods in demography*. Academic Press, San Diego, CA, USA.

Ellner, S.P., Childs, D.Z. & Rees, M. (2016). *Data-driven Modelling of Structured Populations. A practical guide to the Integral Projection Model*. Lecture Notes on Mathematical Modelling in the Life Sciences. Springer International Publishing, Cham.

Evans, M.E.K. & Holsinger, K.E. (2012). Estimating covariation between vital rates : A simulation study of connected vs . separate generalized linear mixed models (GLMMs). *Theor Popul Biol*, 82, 299–306.

Evers, S.M., Knight, T.M., Inouye, D.W., Miller, T.E.X., Salguero-Gómez, R., Iler, A.M., *et al.* (2021). Lagged and dormant season climate better predict plant vital rates than climate during the growing season. *Glob Chang Biol*, 27, 1927–1941.

Fay, R., Hamel, S., van de Pol, M., Gaillard, J.M., Yoccoz, N.G., Acker, P., *et al.* (2022). Temporal correlations among demographic parameters are ubiquitous but highly variable across species. *Ecol Lett*, 25, 1640–1654.

Franco, M. & Silvertown, J. (2004). A comparative demography of plants based upon elasticities of vital rates. *Ecology*, 85, 531–538.

Gaillard, J.M., Festa-Bianchet, M. & Yoccoz, N.G. (1998). Population dynamics of large herbivores: Variable recruitment with constant adult survival. *Trends Ecol Evol*, 13, 58–63.

Gaillard, J.-M. & Yoccoz, N. (2003). Temporal Variation in Survival of Mammals: a Case of Environmental Canalization? *Ecology*, 84, 3294–3306.

Gascoigne, S.J.L., Kajin, M. & Salguero-Gómez, R. (2024a). Criteria for buffering in ecological modeling. *Trends Ecol Evol*, 39, 116–118.

Gascoigne, S.J.L., Kajin, M., Sepil, I. & Salguero-Gómez, R. (2024b). Testing for efficacy in four measures of demographic buffering. *EcoEvoRxiv*, 0–2.

Gascoigne, S.J.L., Kajin, M., Tuljapurkar, S.D., Silva Santos, G., Compagnoni, A., Steiner, U.K., *et al.* (2023a). Structured demographic buffering: A framework to explore the environment drivers and demographic mechanisms underlying demographic buffering. *bioRxiv*.

Gascoigne, S.J.L., Rolph, S., Sankey, D., Nidadavolu, N., Stell Pičman, A.S., Hernández, C.M., *et al.* (2023b). A standard protocol to report discrete stage-structured demographic information. *Methods Ecol Evol*, 14, 2065–2083.

Gillespie, J.H. (1977). Natural Selection for Variances in Offspring Numbers: A New Evolutionary Principle. *Am Nat*, 111, 1010–1014.

Griffith, A.B. (2017). Perturbation approaches for integral projection models. *Oikos*, 126, 1675–1686.

Haridas, C. V. & Tuljapurkar, S. (2005). Elasticities in Variable Environments: Properties and Implications. *Am Nat*, 166, 481–495.

Healy, K., Ezard, T.H.G., Jones, O.R., Salguero-Gómez, R. & Buckley, Y.M. (2019). Animal life history is shaped by the pace of life and the distribution of age-specific mortality and reproduction. *Nat Ecol Evol*, 3, 1217–1224.

Heppell, S.S. (1998). Application of Life-History Theory and Population Model Analysis to Turtle Conservation. *Copeia*, 1998, 367.

Hilde, C.H., Gamelon, M., Sæther, B.-E., Gaillard, J.-M., Yoccoz, N.G. & Pélabon, C. (2020). The Demographic Buffering Hypothesis: Evidence and Challenges. *Trends Ecol Evol*, 35, 523–538.

Jäkäläniemi, A., Ramula, S. & Tuomi, J. (2013). Variability of important vital rates challenges the demographic buffering hypothesis. *Evol Ecol*, 27, 533–545.

Jones, J.H. (2007). demogR: A Package for the Construction and Analysis of Age-structured Demographic Models in R. *J Stat Softw*, 22, 1–28.

Jones, J.H. (2011). Primates and the evolution of long, slow life histories. *Current Biology*, 21, R708–R717.

Jongejans, E., De Kroon, H., Tuljapurkar, S. & Shea, K. (2010). Plant populations track rather than buffer climate fluctuations. *Ecol Lett*, 13, 736–743.

Kajin, M., Gentile, R., Almeida, P.J.A.L. de, Vieira, M.V. & Cerqueira, R. (2023). Vital rates, their variation and natural selection: a case for an Atlantic forest marsupial. *Oecologia Australis*, 27.

Kendall, B.E., Fujiwara, M., Diaz-Lopez, J., Schneider, S., Voigt, J. & Wiesner, S. (2019). Persistent problems in the construction of matrix population models. *Ecol Modell*, 406, 33–43.

Keyfitz, N. & Flieger, W. (1990). *World Population Growth and Aging: Demographic Trends in the Late Twentieth Century*. University of Chicago Press, Chicago.

Koons, D.N., Pavard, S., Baudisch, A. & Jessica E. Metcalf, C. (2009). Is life-history buffering or lability adaptive in stochastic environments? *Oikos*, 118, 972–980.

Kroon, H. De, Groenendaal, J. Van & Ehrlen, J. (2000). Elasticities: A review of methods and model limitations. *Ecology*, 81, 607–618.

de Kroon, H., Plaisier, A., van Groenendaal, J. & Caswell, H. (1986). Elasticity: The Relative Contribution of Demographic Parameters to Population Growth Rate. *Ecology*, 67, 1427–1431.

Lawler, R.R., Caswell, H., Richard, A.F., Ratsirarson, J., Dewar, R.E. & Schwartz, M. (2009). Demography of Verreaux’s sifaka in a stochastic rainfall environment. *Oecologia*, 161, 491–504.

Lefèvre, C.D., Nash, K.L., González-Cabello, A. & Bellwood, D.R. (2016). Consequences of extreme life history traits on population persistence: do short-lived gobies face demographic bottlenecks? *Coral Reefs*, 35, 399–409.

McDonald, J.L., Franco, M., Townley, S., Ezard, T.H.G., Jelbert, K. & Hodgson, D.J. (2017). Divergent demographic strategies of plants in variable environments. *Nat Ecol Evol*, 1, 0029.

Morris, W.F., Altmann, J., Brockman, D.K., Cords, M., Fedigan, L.M., Pusey, A.E., et al. (2011). Low Demographic Variability in Wild Primate Populations: Fitness Impacts of Variation, Covariation, and Serial Correlation in Vital Rates. *Am Nat*, 177, E14–E28.

Morris, W.F. & Doak, D.F. (2004). Buffering of Life Histories against Environmental Stochasticity: Accounting for a Spurious Correlation between the Variabilities of Vital Rates and Their Contributions to Fitness. *Am Nat*, 163, 579–590.



Morris, W.F., Pfister, C.A., Tuljapurkar, S., Haridas, C. V., Boggs, C.L., Boyce, M.S., *et al.* (2008). Longevity can buffer plant and animal populations against changing climatic variability. *Ecology*, 89, 19–25.

Münkemüller, T., Lavergne, S., Bzeznik, B., Dray, S., Jombart, T., Schiffrers, K., *et al.* (2012). How to measure and test phylogenetic signal. *Methods Ecol Evol*, 3, 743–756.

Pélabon, C., Hilde, C.H., Einum, S. & Gamelon, M. (2020). On the use of the coefficient of variation to quantify and compare trait variation. *Evol Lett*, 4, 180–188.

Perret, D.L., Evans, M.E.K. & Sax, D.F. (2024). A species' response to spatial climatic variation does not predict its response to climate change. *Proc Natl Acad Sci U S A*, 121, e2304404120.

Pfister, C. (1998). Patterns of variance in stage-structured populations: Evolutionary predictions and ecological implications. *Proceedings of the National Academy of Sciences*, 95, 213–218.

R Core Team. (2024). R: A Language and Environment for Statistical Computing.

Reed, A.W. & Slade, N.A. (2012). Buffering and plasticity in vital rates of oldfield rodents. *Journal of Animal Ecology*, 81, 953–959.

Rodríguez-Caro, R.C., Capdevila, P., Graciá, E., Barbosa, J.M., Giménez, A. & Salguero-Gómez, R. (2021). The limits of demographic buffering in coping with environmental variation. *Oikos*, 130, 1346–1358.

Römer, G., Dahlgren, J.P., Salguero-Gómez, R., Stott, I.M. & Jones, O.R. (2024). Plant demographic knowledge is biased towards short-term studies of temperate-region herbaceous perennials. *Oikos*, 2024.

Rotella, J.J., Link, W.A., Chambert, T., Stauffer, G.E. & Garrott, R.A. (2012). Evaluating the demographic buffering hypothesis with vital rates estimated for Weddell seals from 30 years of mark-recapture data. *Journal of Animal Ecology*, 81, 162–173.

Salguero-Gómez, R. (2021). Commentary on the life history special issue: The fast-slow continuum is not the end-game of life history evolution, human or otherwise. *Evolution and Human Behavior*, 42, 281–283.

Salguero-Gómez, R. (2024). More social species live longer, have higher generation times, and longer reproductive windows. *bioRxiv*; <https://doi.org/10.1101/2024.01.22.575897>.

Salguero-Gómez, R., Jackson, J. & Gascoigne, S.J.L. (2021). Four key challenges in the open-data revolution. *Journal of Animal Ecology*, 90, 2000–2004.

Salguero-Gómez, R., Jones, O.R., Archer, C.R., Bein, C., de Buhr, H., Farack, C., *et al.* (2016). COMADRE: A global data base of animal demography. *Journal of Animal Ecology*, 85, 371–384.

Sanghvi, K., Vega-Trejo, R., Nakagawa, S., Gascoigne, S.J.L., Johnson, S.L., Salguero-Gómez, R., *et al.* (2024). Meta-analysis shows no consistent evidence for senescence in ejaculate traits across animals. *Nat Commun*, 15, 558.

Shyu, E. & Caswell, H. (2014). Calculating second derivatives of population growth rates for ecology and evolution. *Methods Ecol Evol*, 5, 473–482.

Simmonds, E.G. & Jones, O.R. (2024). Uncertainty propagation in matrix population models: Gaps, importance and guidelines. *Methods Ecol Evol*, 15, 427–438.

Stearns, S. (1992). *The Evolution of Life Histories*. Oxford University Press, New York, USA.

Stearns, S.C. (1983). The Influence of Size and Phylogeny on Patterns of Covariation among Life-History Traits in the Mammals. *Oikos*, 41, 173.

Stubben, C., Milligan, B., Nantel, P. & Stubben, M.C. (2020). Package ‘popbio.’

Sutherland, W.J., Freckleton, R.P., Godfray, H.C.J., Beissinger, S.R., Benton, T., Cameron, D.D., *et al.* (2013). Identification of 100 fundamental ecological questions. *Journal of Ecology*, 101, 58–67.

1514 [Tuljapurkar, S. \(1990\). Population Dynamics in Variable Environments. In: \*Lecture notes in\*](#)  
1515 [Biomathematics](#), Lecture Notes in Biomathematics (ed. Levin, S.). Springer Berlin  
1516 [Heidelberg.](#)

1517 [Tuljapurkar, S. \(2010\). Environmental variance, population growth and evolution. \*J Anim\*](#)  
1518 [Ecol](#), 79, 1–3.

1519 [Tuljapurkar, S., Gaillard, J.-M. & Coulson, T. \(2009\). From stochastic environments to life](#)  
1520 [histories and back. \*Philosophical Transactions of the Royal Society B: Biological\*](#)  
1521 [Sciences](#), 364, 1499–1509.

1522 [Tuljapurkar, S., Horvitz, C.C. & Pascarella, J.B. \(2003\). The Many Growth Rates and](#)  
1523 [Elasticities of Populations in Random Environments. \*Am Nat\*](#), 162, 489–502.

1524 [Tuljapurkar, S., Jaggi, H., Gascoigne, S.J.L., Zuo, W., Kajin, M. & Salguero-Gómez, R.](#)  
1525 [\(2023\). From disturbances to nonlinear fitness and back. \*bioRxiv\*, 2023.10.20.563360.](#)

1526 [Tuljapurkar, S.D. \(1982\). Population dynamics in variable environments. III. Evolutionary](#)  
1527 [dynamics of r-selection. \*Theor Popul Biol\*](#), 21, 141–165.

1528 [Vázquez, D.P., Gianoli, E., Morris, W.F. & Bozinovic, F. \(2017\). Ecological and](#)  
1529 [evolutionary impacts of changing climatic variability. \*Biological Reviews\*](#), 92, 22–42.

1530 [Wang, J., Yang, X., Silva Santos, G., Ning, H., Li, T., Zhao, W., \*et al.\* \(2023\). Flexible](#)  
1531 [demographic strategies promote the population persistence of a pioneer conifer tree](#)  
1532 [\(\*Pinus massoniana\*\) in ecological restoration. \*For Ecol Manage\*](#), 529, 120727.

1533 [Zuidema, P.A. & Franco, M. \(2001\). Integrating vital rate variability into perturbation](#)  
1534 [analysis: an evaluation for matrix population models of six plant species. \*Journal of\*](#)  
1535 [Ecology](#), 89, 995–1005.

1536 -

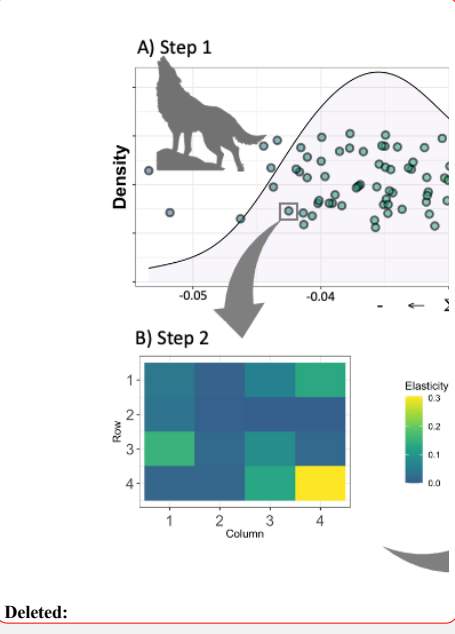
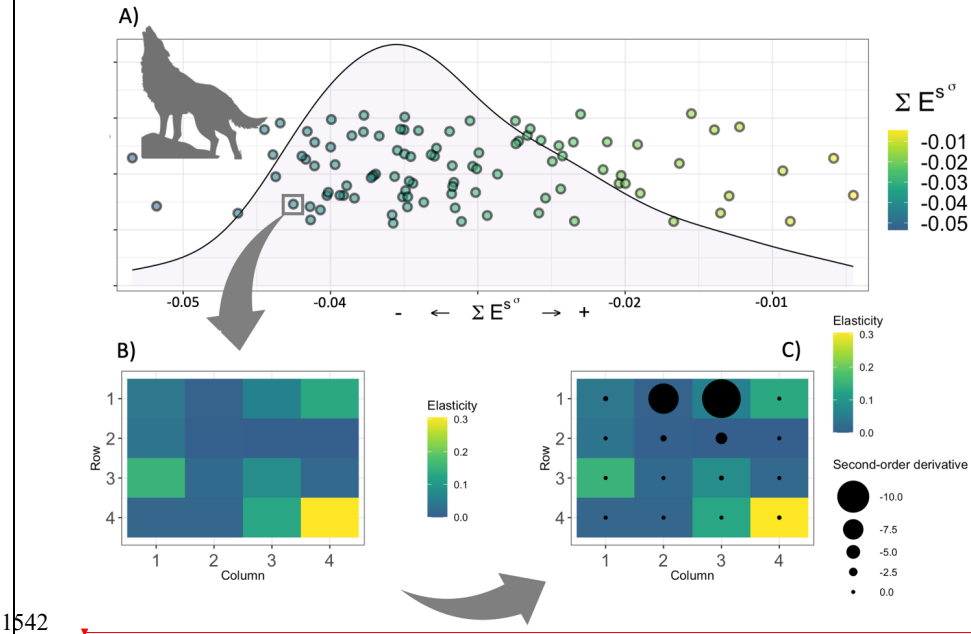
1537

1538

1539

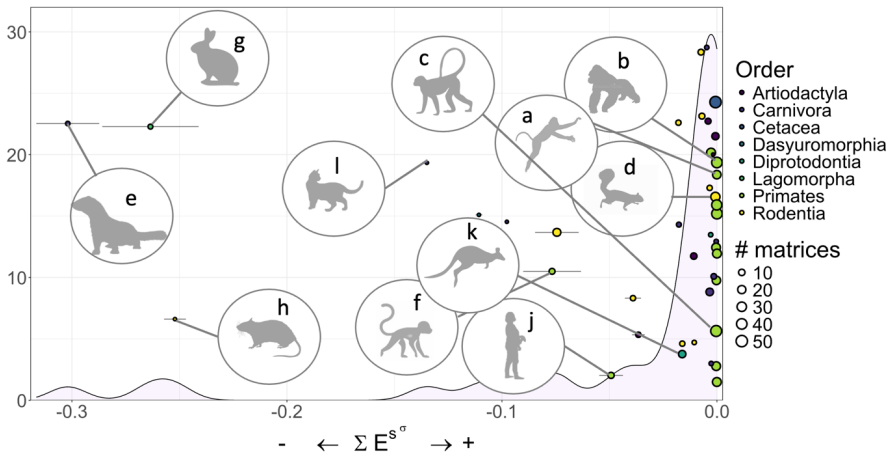
1540

1541 **Figure 1**



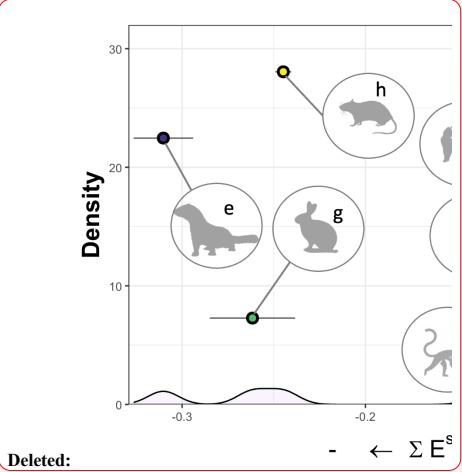
1544

Figure 2

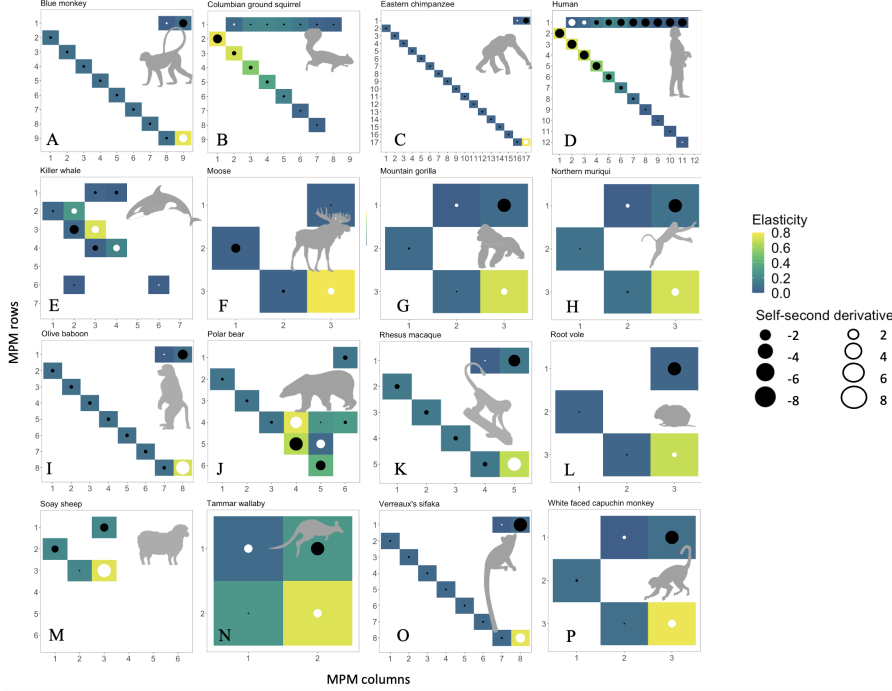


1545

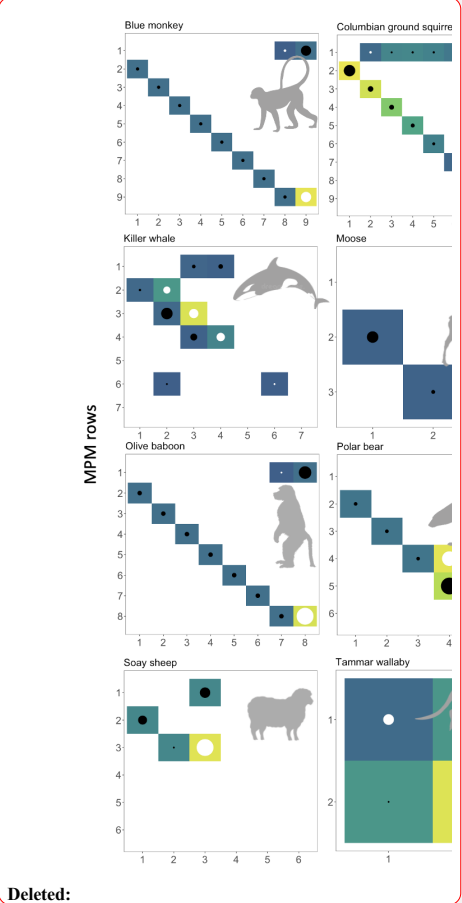
1546



1548 **Figure 3**



1549  
1550  
1551



Deleted:

## Figure legends

**Figure 1.** A) The variance continuum for 37 hypothetical species based on the summed stochastic elasticities ( $\Sigma E_{aij}^{S\sigma}$ ) at the between populations hierarchical level. The closer the  $\Sigma E_{aij}^{S\sigma}$  is to zero, the weaker the impact of variation in demographic processes on the stochastic population growth rate,  $\lambda_s$ . The variance continuum ranges from potentially buffered (right-hand side) to less buffered (left-hand side) species/populations. The yellow-dotted species/populations can be classified as having potentially buffered life cycles. The left-hand side of the graph represents species/populations where variability in demographic processes results in strong impact on  $\lambda_s$  (blue dots). Thus, the blue-dotted species/populations can be classified as having potentially unbuffered life cycles. The vertical axis delineates the values of the probability density function, indicating the number of species/populations at each value of  $\Sigma E_{aij}^{S\sigma}$ . The placement of data points (species/populations) along the horizontal axis corresponds to their calculated values of  $\Sigma E_{aij}^{S\sigma}$  and is arranged linearly, while the placement along the y-axis is random for improved visual comprehension. B) First-order effects or linear selection pressures for individual species/populations at within-species level (see text). Shown are the elasticities of the deterministic population growth rate ( $\lambda_d$ ) for a hypothetical population of wolves and revealing the governing demographic process(es) in the life cycle (yellow cells: high elasticity, blue cells: low elasticity). C) Combined results for first (yellow and blue cells) and second order effects (black dots), where the latter reveals the nonlinear selection pressures at the within-species level.

**Figure 2.** The variance continuum for 43 populations from 37 species of mammals from the COMADRE database based on the summed stochastic elasticities ( $\Sigma E_{aij}^{S\sigma}$ ) at the between populations hierarchical level. Colors represent different taxonomic orders with Primates occupying the right-hand side. Silhouettes: a) *Brachyteles hypoxantus*, b) *Gorilla beringhei*,

- Deleted: A three-step framework proposed to: Step
- Deleted: 1 - allocate species and/or populations on a
- Deleted: (plot A, dots representing
- Deleted: 50
- Deleted: )
- Deleted: The variance continuum operates at the between-populations level (see text) and is represented by partitioning the sum of all the stochastic elasticities into two compounds: i) sums of stochastic elasticities with resp (... [34]
- Deleted: (or
- Deleted: )
- Deleted: -
- Deleted: - based on all the demographic processes
- Deleted: (or
- Deleted: )
- Deleted: a perturbation of the variance
- Deleted: (or
- Deleted: )
- Deleted: - based on all the demographic processes
- Deleted: distribution
- Deleted: breadth
- Deleted: solely
- Deleted: Step
- Deleted: 2 -
- Deleted:
- Deleted: Access the
- Deleted: or
- Deleted: (plot B)
- Deleted: Step 2
- Deleted: displays
- Deleted:  $\lambda$
- Deleted: wolf
- Deleted: s
- Deleted: linear selection gradients
- Deleted: ,
- Deleted: and which demographic processes are the m (... [35]
- Deleted:  $\lambda_t$
- Deleted: Step 3
- Deleted: -
- Deleted: Access the n
- Deleted: (see text) (plot C)
- Deleted: In the third step self-second derivatives for t (... [36]
- Deleted: 40
- Deleted: 34
- Deleted: Results for step 1 of our framework showing (... [37]

c) *Cercopithecus mitis*, d) *Urocyon v. columbianus*, e) *Mustela erminea*, f) *Erythrocebus patas*, g) *Lepus americanus*, h) *Rattus fuscipes*, i) *Ovis aries*, j) *Homo sapiens*, k) *Macropus eugenii*, and l) *Felis catus*. The vertical axis delineates the values of the probability density function, indicating the number of species/populations at each value of  $\Sigma E_{a_{ij}}^{\sigma}$ . The placement of data points (species/populations) along the horizontal axis corresponds to their calculated values of  $\Sigma E_{a_{ij}}^{\sigma}$  and is arranged linearly, while the **placement** along the y-axis is **random** for improved visual comprehension.

**Figure 3: First and second order effects on population growth rate,  $\lambda_l$  (corresponding to elasticities and self-second derivatives of population growth rate, respectively) for 16 mammal species.** The 16 plots represent populations where the MPMs built by ages were available in the COMADRE *Animal Matrix Database*. The **yellow-blue colour** scale represents elasticity values for each of the demographic processes in the MPM, where yellow cells represent high and blue cells low elasticity of population growth rate to changes in demographic processes. No colour means elasticity=0. The black dots represent negative self-second derivatives of  $\lambda_l$  - corresponding to concave selection - and the white dots represent positive self-second derivatives of  $\lambda_l$  - ditto convex selection. The dot sizes are scaled by the absolute value of self-second derivatives, where the smaller the dot, the closer a self-second derivative is to 0, indicating weak or no nonlinearity. Thus, large dots indicate strong nonlinear selection forces, either concave (black) or convex (white). Since the derivatives of population growth rate are confounded by eigen-structure (Kroon *et al.* 2000), the scaling of the elasticity values and second-derivative values is species specific - i.e., each plot has its own scale. Species-specific scales can be found in Supplementary material (Table S2).

Deleted: breadth

Deleted: solely

Deleted: Results from steps 2 and 3 of the proposed framework (see Fig. 2B, C).

Deleted: d

Deleted: (see text)

Deleted: color

Deleted: s

Deleted: values.

Deleted: color

Deleted: Because the aim of step 2 is to identify the most impacting demographic process within each species' life cycle (the within-populations level, see text) - not to compare the elasticity values among species - each plot has its own scale (see end of legend).

Deleted: The black dots represent negative self-second derivatives of  $\lambda_l$  - thus concave selection - and the white dots represent positive self-second derivatives of  $\lambda_l$  - thus convex selection. The dot sizes are scaled by the absolute value of self-second derivatives, where the smaller the dot, the closer a self-second derivative is to 0, indicating weak or no nonlinearity. Large dots indicate strong nonlinear selection forces. Scales ( $E_{\min-\max}$ =elasticity minimum and maximum value,  $SSD_{\min-\max}$ =self-second derivative minimum and maximum value): Blue monkey  $E_{\min-\max}=0.00-0.52$ ,  $SSD_{\min-\max}=-1.25-1.27$ ; Columbian ground squirrel:  $E_{\min-\max}=0.00-0.23$ ,  $SSD_{\min-\max}=-1.48-0.01$ ; Eastern chimpanzee:  $E_{\min-\max}=0.00-0.60$ ,  $SSD_{\min-\max}=-4.39-2.59$ ; Human:  $E_{\min-\max}=0.00-0.18$ ,  $SSD_{\min-\max}=-0.15-0.08$ ; Killer whale:  $E_{\min-\max}=0.00-0.55$ ,  $SSD_{\min-\max}=-5.72-3.43$ ; Moose:  $E_{\min-\max}=0.00-0.55$ ,  $SSD_{\min-\max}=-0.66-0.36$ ; Mountain gorilla:  $E_{\min-\max}=0.00-0.81$ ,  $SSD_{\min-\max}=-1.46-0.28$ ; Northern muriqui:  $E_{\min-\max}=0.00-0.72$ ,  $SSD_{\min-\max}=-1.17-0.35$ ; Olive baboon:  $E_{\min-\max}=0.00-0.54$ ,  $SSD_{\min-\max}=-0.57-1.13$ ; Polar bear:  $E_{\min-\max}=0.00-0.26$ ,  $SSD_{\min-\max}=-0.73-0.54$ ; Rhesus macaque:  $E_{\min-\max}=0.00-0.51$ ,  $SSD_{\min-\max}=-0.54-0.71$ ; Root vole:  $E_{\min-\max}=0.00-0.86$ ,  $SSD_{\min-\max}=-2.54-0.22$ ; Soay sheep:  $E_{\min-\max}=0.00-0.56$ ,  $SSD_{\min-\max}=-0.22-0.40$ ; Tammar wallaby:  $E_{\min-\max}=0.00-0.55$ ,  $SSD_{\min-\max}=-0.64-0.34$ ; Verreaux's sifaka:  $E_{\min-\max}=0.00-0.60$ ,  $SSD_{\min-\max}=-2.64-1.34$ ; White faced capuchin monkey:  $E_{\min-\max}=0.00-0.66$ ,  $SSD_{\min-\max}=-2.66-1.21$ .



**Supplementary material – Data available in COMADRE Version 3.0.0 and results from Step 1 of the framework**

**Table S1.** The metadata used and the respective results presented in the main text. The first four columns represent the information from where

Matrix Populations Models (MPMs) were extract precisely as presented in COMADRE 3.0.0.

<u>Species</u>	<u>Common name</u>	<u>Species (COMADRE)</u>	<u>Order</u>	<u># matrices</u>	$\lambda_l$	$\lambda_s$	$\Sigma E_{a_{ij}}^{s\sigma}$	$\Sigma E_{a_{ij}}^{s\sigma}(\text{SE})$
<u><i>Homo sapiens sapiens</i></u>	<u>Human</u>	<u>Homo_sapiens_sub sp. sapiens</u>	<u>Primates</u>	<u>26</u>	<u>1.063707</u>	<u>1.061537</u>	<u>-2.24E-03</u>	<u>3.15E-04</u>
<u><i>Alces alces</i></u>	<u>Moose</u>	<u>Alces_alces</u>	<u>Artiodactyla</u>	<u>14</u>	<u>1.205368</u>	<u>1.205161</u>	<u>-6.69E-04</u>	<u>8.42E-05</u>
<u><i>Antechinus agilis</i></u>	<u>Agile antechinus</u>	<u>Antechinus_agilis</u>	<u>Dasyuromorphia</u>	<u>3</u>	<u>0.931076</u>	<u>0.885919</u>	<u>-1.11E-01</u>	<u>1.62E-03</u>
<u><i>Bos primigenius</i></u>	<u>Cattle</u>	<u>Bos_primigenius</u>	<u>Artiodactyla</u>	<u>8</u>	<u>1.002505</u>	<u>1.000493</u>	<u>-2.83E-03</u>	<u>2.96E-04</u>
<u><i>Brachyteles hypoxanthus</i></u>	<u>Northern muriqui</u>	<u>Brachyteles_hypoxanthus</u>	<u>Primates</u>	<u>25</u>	<u>1.05122</u>	<u>1.051273</u>	<u>-5.31E-05</u>	<u>2.09E-05</u>
<u><i>Callospermophilus lateralis</i></u>	<u>Golden-mantled ground squirrel</u>	<u>Callospermophilus_lateralis</u>	<u>Rodentia</u>	<u>18</u>	<u>2.052345</u>	<u>1.970253</u>	<u>-6.68E-02</u>	<u>8.72E-03</u>
<u><i>Cebus capucinus</i></u>	<u>White faced capuchin monkey</u>	<u>Cebus_capucinus</u>	<u>Primates</u>	<u>22</u>	<u>1.020887</u>	<u>1.020868</u>	<u>-2.04E-04</u>	<u>4.75E-05</u>
<u><i>Cercopithecus mitis</i></u>	<u>Blue monkey</u>	<u>Cercopithecus_mitis</u>	<u>Primates</u>	<u>28</u>	<u>1.036082</u>	<u>1.036075</u>	<u>-4.43E-05</u>	<u>1.18E-05</u>

**Deleted:** in step 1 of our framework

**Deleted:** 2

**Deleted:** 1

**Deleted:** Column titles differ from the database as “SpeciesAuthorComadre” is equivalent to “SpeciesAuthor” and “SpeciesName” is equivalent to “SpeciesAccepted” in COMADRE 3.0.0. The remaining columns present the results of step 1, where we present the raw values of  $\lambda$ , their respective standard deviation, the stochastic population growth rate  $\lambda_s$ , and the number of available matrices (# matrices).

<a href="#"><u>Cervus canadensis subsp. nelsoni</u></a>	<a href="#"><u>Rocky Mountain elk</u></a>	<a href="#"><u>Cervus canadensis subsp. nelsoni</u></a>	<a href="#"><u>Artiodactyla</u></a>	<a href="#"><u>10</u></a>	<a href="#"><u>1.107412</u></a>	<a href="#"><u>1.099838</u></a>	<a href="#"><u>-8.55E-03</u></a>	<a href="#"><u>1.09E-03</u></a>
<a href="#"><u>Eumetopias jubatus</u></a>	<a href="#"><u>Northern sea lion; Steller sea lion</u></a>	<a href="#"><u>Eumetopias jubatus</u></a>	<a href="#"><u>Carnivora</u></a>	<a href="#"><u>4</u></a>	<a href="#"><u>0.904383</u></a>	<a href="#"><u>0.902155</u></a>	<a href="#"><u>-4.52E-03</u></a>	<a href="#"><u>2.44E-04</u></a>
<a href="#"><u>Felis catus</u></a>	<a href="#"><u>Feral cat</u></a>	<a href="#"><u>Felis catus</u></a>	<a href="#"><u>Carnivora</u></a>	<a href="#"><u>3</u></a>	<a href="#"><u>1.948471</u></a>	<a href="#"><u>1.8259</u></a>	<a href="#"><u>-1.34E-01</u></a>	<a href="#"><u>1.89E-03</u></a>
<a href="#"><u>Gorilla beringei</u></a>	<a href="#"><u>Mountain gorilla</u></a>	<a href="#"><u>Gorilla beringei</u></a>	<a href="#"><u>Primates</u></a>	<a href="#"><u>41</u></a>	<a href="#"><u>1.026827</u></a>	<a href="#"><u>1.02682</u></a>	<a href="#"><u>-1.28E-05</u></a>	<a href="#"><u>1.32E-05</u></a>
<a href="#"><u>Hippocamelus bisulcus</u></a>	<a href="#"><u>Huemul deer</u></a>	<a href="#"><u>Hippocamelus bisulcus</u></a>	<a href="#"><u>Artiodactyla</u></a>	<a href="#"><u>3</u></a>	<a href="#"><u>0.996197</u></a>	<a href="#"><u>0.995462</u></a>	<a href="#"><u>-1.80E-03</u></a>	<a href="#"><u>1.09E-04</u></a>
<a href="#"><u>Leopardus pardalis</u></a>	<a href="#"><u>Ocelot</u></a>	<a href="#"><u>Leopardus pardalis</u></a>	<a href="#"><u>Carnivora</u></a>	<a href="#"><u>4</u></a>	<a href="#"><u>1.086146</u></a>	<a href="#"><u>1.086122</u></a>	<a href="#"><u>-2.94E-04</u></a>	<a href="#"><u>3.89E-05</u></a>
<a href="#"><u>Lepus americanus</u></a>	<a href="#"><u>Snowshoe hare</u></a>	<a href="#"><u>Lepus americanus</u></a>	<a href="#"><u>Lagomorpha</u></a>	<a href="#"><u>5</u></a>	<a href="#"><u>0.811904</u></a>	<a href="#"><u>0.707678</u></a>	<a href="#"><u>-2.62E-01</u></a>	<a href="#"><u>2.33E-02</u></a>
<a href="#"><u>Lycaon pictus</u></a>	<a href="#"><u>African wild dog</u></a>	<a href="#"><u>Lycaon pictus</u></a>	<a href="#"><u>Carnivora</u></a>	<a href="#"><u>3</u></a>	<a href="#"><u>1.500429</u></a>	<a href="#"><u>1.430517</u></a>	<a href="#"><u>-9.70E-02</u></a>	<a href="#"><u>9.91E-04</u></a>
<a href="#"><u>Macaca mulatta</u></a>	<a href="#"><u>Rhesus macaque</u></a>	<a href="#"><u>Macaca mulatta_3</u></a>	<a href="#"><u>Primates</u></a>	<a href="#"><u>24</u></a>	<a href="#"><u>1.127496</u></a>	<a href="#"><u>1.12735</u></a>	<a href="#"><u>-3.84E-04</u></a>	<a href="#"><u>6.83E-05</u></a>
<a href="#"><u>Macropus eugenii</u></a>	<a href="#"><u>Tammar wallaby</u></a>	<a href="#"><u>Macropus eugenii</u></a>	<a href="#"><u>Diprotodontia</u></a>	<a href="#"><u>15</u></a>	<a href="#"><u>0.981097</u></a>	<a href="#"><u>0.970794</u></a>	<a href="#"><u>-1.43E-02</u></a>	<a href="#"><u>1.62E-03</u></a>
<a href="#"><u>Marmota flaviventris</u></a>	<a href="#"><u>Yellow-bellied marmot</u></a>	<a href="#"><u>Marmota flaviventris_2</u></a>	<a href="#"><u>Rodentia</u></a>	<a href="#"><u>8</u></a>	<a href="#"><u>0.89031</u></a>	<a href="#"><u>0.886098</u></a>	<a href="#"><u>-8.80E-03</u></a>	<a href="#"><u>6.98E-04</u></a>
<a href="#"><u>Marmota flaviventris</u></a>	<a href="#"><u>Yellow-bellied marmot</u></a>	<a href="#"><u>Marmota flaviventris_3</u></a>	<a href="#"><u>Rodentia</u></a>	<a href="#"><u>8</u></a>	<a href="#"><u>0.920541</u></a>	<a href="#"><u>0.916392</u></a>	<a href="#"><u>-7.00E-03</u></a>	<a href="#"><u>7.04E-04</u></a>

<a href="#">Microtus oeconomus</a>	<a href="#">Root vole</a>	<a href="#">Microtus oeconomus</a>	<a href="#">Rodentia</a>	<a href="#">28</a>	<a href="#">1.027531</a>	<a href="#">1.027095</a>	<a href="#">-5.60E-04</a>	<a href="#">1.06E-04</a>
<a href="#">Mustela erminea</a>	<a href="#">Stoat</a>	<a href="#">Mustela erminea</a>	<a href="#">Carnivora</a>	<a href="#">4</a>	<a href="#">1.258462</a>	<a href="#">1.074391</a>	<a href="#">-3.10E-01</a>	<a href="#">1.62E-02</a>
<a href="#">Orcinus orca</a>	<a href="#">Killer whale</a>	<a href="#">Orcinus orca_2</a>	<a href="#">Cetacea</a>	<a href="#">50</a>	<a href="#">0.998658</a>	<a href="#">0.998351</a>	<a href="#">-4.72E-04</a>	<a href="#">1.53E-04</a>
<a href="#">Ovis aries</a>	<a href="#">Soay sheep</a>	<a href="#">Ovis aries_2</a>	<a href="#">Artiodactyla</a>	<a href="#">6</a>	<a href="#">1.09877</a>	<a href="#">1.080656</a>	<a href="#">-3.45E-02</a>	<a href="#">2.96E-03</a>
<a href="#">Pan troglodytes subsp. schweinfurthii</a>	<a href="#">Eastern chimpanzee</a>	<a href="#">Pan troglodytes subsp. schweinfurthii</a>	<a href="#">Primates</a>	<a href="#">45</a>	<a href="#">0.982286</a>	<a href="#">0.982191</a>	<a href="#">-1.94E-04</a>	<a href="#">5.06E-05</a>
<a href="#">Papio cynocephalus</a>	<a href="#">Olive baboon</a>	<a href="#">Papio cynocephalus</a>	<a href="#">Primates</a>	<a href="#">37</a>	<a href="#">1.053872</a>	<a href="#">1.053789</a>	<a href="#">-2.41E-04</a>	<a href="#">6.97E-05</a>
<a href="#">Peromyscus maniculatus</a>	<a href="#">Deer mouse</a>	<a href="#">Peromyscus maniculatus_2</a>	<a href="#">Rodentia</a>	<a href="#">4</a>	<a href="#">1.10686</a>	<a href="#">1.101117</a>	<a href="#">-9.41E-03</a>	<a href="#">6.88E-04</a>
<a href="#">Phascolarctos cinereus</a>	<a href="#">Koala</a>	<a href="#">Phascolarctos cinereus_2</a>	<a href="#">Diprotodontia</a>	<a href="#">4</a>	<a href="#">1.064011</a>	<a href="#">1.062744</a>	<a href="#">-2.53E-03</a>	<a href="#">2.16E-04</a>
<a href="#">Phocarcos hookeri</a>	<a href="#">New Zealand sea lion</a>	<a href="#">Phocarcos hookeri</a>	<a href="#">Carnivora</a>	<a href="#">16</a>	<a href="#">1.023016</a>	<a href="#">1.020083</a>	<a href="#">-3.56E-03</a>	<a href="#">4.15E-04</a>
<a href="#">Propithecus verreauxi</a>	<a href="#">Verreaux's sifaka</a>	<a href="#">Propithecus verreauxi</a>	<a href="#">Primates</a>	<a href="#">24</a>	<a href="#">0.985592</a>	<a href="#">0.985399</a>	<a href="#">-3.06E-04</a>	<a href="#">6.29E-05</a>
<a href="#">Rattus fuscipes</a>	<a href="#">Bush rat</a>	<a href="#">Rattus fuscipes</a>	<a href="#">Rodentia</a>	<a href="#">3</a>	<a href="#">1.304662</a>	<a href="#">1.188931</a>	<a href="#">-2.45E-01</a>	<a href="#">4.29E-03</a>
<a href="#">Uroditellus armatus</a>	<a href="#">Uinta ground squirrel</a>	<a href="#">Spermophilus armatus</a>	<a href="#">Rodentia</a>	<a href="#">6</a>	<a href="#">1.125011</a>	<a href="#">1.113416</a>	<a href="#">-1.73E-02</a>	<a href="#">1.68E-03</a>

<u>Urocyon</u> <u>armatus</u>	<u>Uta ground</u> <u>squirrel</u>	<u>Spermophilus arm</u> <u>atus 2</u>	<u>Rodentia</u>	<u>6</u>	<u>1.094693</u>	<u>1.084304</u>	<u>-1.47E-02</u>	<u>1.56E-03</u>
<u>Urocyon</u> <u>columbianus</u>	<u>Columbian ground</u> <u>squirrel</u>	<u>Spermophilus colu</u> <u>mbianus</u>	<u>Rodentia</u>	<u>6</u>	<u>1.008949</u>	<u>0.984575</u>	<u>-3.80E-02</u>	<u>3.26E-03</u>
<u>Urocyon</u> <u>columbianus</u>	<u>Columbian ground</u> <u>squirrel</u>	<u>Spermophilus colu</u> <u>mbianus 3</u>	<u>Rodentia</u>	<u>6</u>	<u>1.200353</u>	<u>1.197473</u>	<u>-3.38E-03</u>	<u>6.96E-04</u>
<u>Ursus</u> <u>americanus</u> <u>subsp. floridanus</u>	<u>Florida black bear</u>	<u>Ursus americanus</u> <u>subsp. floridanus</u>	<u>Carnivora</u>	<u>4</u>	<u>1.01989</u>	<u>1.018094</u>	<u>-3.68E-03</u>	<u>3.97E-04</u>
<u>Ursus arctos</u> <u>subsp. horribilis</u>	<u>Grizzly bear</u>	<u>Ursus arctos subs</u> <u>p. horribilis 5</u>	<u>Carnivora</u>	<u>7</u>	<u>1.025712</u>	<u>1.024785</u>	<u>-1.38E-03</u>	<u>1.26E-04</u>
<u>Ursus maritimus</u>	<u>Polar bear</u>	<u>Ursus maritimus 2</u>	<u>Carnivora</u>	<u>5</u>	<u>0.940646</u>	<u>0.931697</u>	<u>-1.91E-02</u>	<u>9.23E-04</u>
<u>Brachyteles</u> <u>hypoxanthus</u>	<u>Northern muriqui</u>	<u>Brachyteles hypox</u> <u>anthus 2</u>	<u>Primates</u>	<u>25</u>	<u>1.110953</u>	<u>1.110983</u>	<u>1.22E-05</u>	<u>5.05E-06</u>
<u>Cebus capucinus</u>	<u>White-faced</u> <u>capuchin monkey</u>	<u>Cebus capucinus</u> <u>2</u>	<u>Primates</u>	<u>22</u>	<u>1.059311</u>	<u>1.059248</u>	<u>-1.03E-04</u>	<u>2.85E-05</u>
<u>Chlorocebus</u> <u>aethiops</u>	<u>Vervet</u>	<u>Chlorocebus aethi</u> <u>ops 2</u>	<u>Primates</u>	<u>8</u>	<u>1.187136</u>	<u>1.148862</u>	<u>-8.03E-02</u>	<u>1.31E-02</u>
<u>Erythrocebus</u> <u>patas</u>	<u>Patas monkey</u>	<u>Erythrocebus patas</u>	<u>Primates</u>	<u>9</u>	<u>1.127974</u>	<u>1.092178</u>	<u>-5.21E-02</u>	<u>5.38E-03</u>
<u>Gorilla beringei</u> <u>subsp. beringei</u>	<u>Mountain gorilla</u>	<u>Gorilla beringei s</u> <u>ubsp. beringei</u>	<u>Primates</u>	<u>41</u>	<u>1.052588</u>	<u>1.05255</u>	<u>-6.81E-05</u>	<u>1.11E-05</u>

**Table S2.** The species-specific scales for the elasticity of  $\lambda_I$  to changes in demographic processes and for the self-second derivatives of  $\lambda_I$  with respect to demographic processes for the 16 mammal species studied.

<u>Figure 3 reference</u>	<u>Species common name</u>	<u>E<sub>min</sub>=elasticity minimum value</u>	<u>E<sub>max</sub>=elasticity maximum value</u>	<u>SSD<sub>min</sub>=self-second derivative minimum value</u>	<u>SSD<sub>max</sub>=self-second derivative maximum value</u>
<u>A</u>	<u>Blue monkey</u>	<u>0</u>	<u>0.52</u>	<u>-1.25</u>	<u>1.27</u>
<u>B</u>	<u>Columbian ground squirrel</u>	<u>0</u>	<u>0.23</u>	<u>-1.48</u>	<u>0.01</u>
<u>C</u>	<u>Eastern chimpanzee</u>	<u>0</u>	<u>0.60</u>	<u>-4.39</u>	<u>2.59</u>
<u>D</u>	<u>Human</u>	<u>0</u>	<u>0.18</u>	<u>-0.15</u>	<u>0.08</u>
<u>E</u>	<u>Killer whale</u>	<u>0</u>	<u>0.55</u>	<u>-5.72</u>	<u>3.43</u>
<u>F</u>	<u>Moose</u>	<u>0</u>	<u>0.55</u>	<u>-0.66</u>	<u>0.36</u>
<u>G</u>	<u>Mountain gorilla</u>	<u>0</u>	<u>0.81</u>	<u>-1.46</u>	<u>0.28</u>
<u>H</u>	<u>Northern muriqui</u>	<u>0</u>	<u>0.72</u>	<u>-1.17</u>	<u>0.35</u>
<u>I</u>	<u>Olive baboon</u>	<u>0</u>	<u>0.54</u>	<u>-0.57</u>	<u>1.13</u>
<u>J</u>	<u>Polar bear</u>	<u>0</u>	<u>0.26</u>	<u>-0.73</u>	<u>0.54</u>
<u>K</u>	<u>Rhesus macaque</u>	<u>0</u>	<u>0.51</u>	<u>-0.54</u>	<u>0.71</u>
<u>L</u>	<u>Root vole</u>	<u>0</u>	<u>0.86</u>	<u>-2.54</u>	<u>0.22</u>
<u>M</u>	<u>Soay sheep</u>	<u>0</u>	<u>0.56</u>	<u>-0.22</u>	<u>0.40</u>
<u>N</u>	<u>Tammar wallaby</u>	<u>0</u>	<u>0.55</u>	<u>-0.64</u>	<u>0.34</u>
<u>O</u>	<u>Verreaux's sifaka</u>	<u>0</u>	<u>0.60</u>	<u>-2.64</u>	<u>1.34</u>
<u>P</u>	<u>White faced capuchin monkey</u>	<u>0</u>	<u>0.66</u>	<u>-2.66</u>	<u>1.21</u>